



**HAL**  
open science

# On the data completion problem and the inverse obstacle problem with partial Cauchy data for Laplace's equation

Fabien Caubet, Jérémie Dardé, Matías Godoy

## ► To cite this version:

Fabien Caubet, Jérémie Dardé, Matías Godoy. On the data completion problem and the inverse obstacle problem with partial Cauchy data for Laplace's equation. *ESAIM: Control, Optimisation and Calculus of Variations*, 2017, 10.1051/cocv/2017056 . hal-01624524

**HAL Id: hal-01624524**

**<https://hal.science/hal-01624524v1>**

Submitted on 26 Oct 2017

**HAL** is a multi-disciplinary open access archive for the deposit and dissemination of scientific research documents, whether they are published or not. The documents may come from teaching and research institutions in France or abroad, or from public or private research centers.

L'archive ouverte pluridisciplinaire **HAL**, est destinée au dépôt et à la diffusion de documents scientifiques de niveau recherche, publiés ou non, émanant des établissements d'enseignement et de recherche français ou étrangers, des laboratoires publics ou privés.

# On the data completion problem and the inverse obstacle problem with partial Cauchy data for Laplace's equation

Fabien Caubet\*, Jérémie Dardé† and Matías Godoy‡

June 21, 2017

## Abstract

We study the inverse problem of obstacle detection for Laplace's equation with partial Cauchy data. The strategy used is to reduce the inverse problem into the minimization of a cost-type functional: the Kohn-Vogelius functional. Since the boundary conditions are unknown on an inaccessible part of the boundary, the variables of the functional are the shape of the inclusion but also the Cauchy data on the inaccessible part. Hence we first focus on recovering these boundary conditions, *i.e.* on the data completion problem. Due to the ill-posedness of this problem, we regularize the functional through a Tikhonov regularization. Then we obtain several theoretical properties for this data completion problem, as convergence properties, in particular when data are corrupted by noise. Finally, we propose an algorithm to solve the inverse obstacle problem with partial Cauchy data by minimizing the Kohn-Vogelius functional. Thus we obtain the gradient of the functional computing both the derivatives with respect to the missing data and to the shape. Several numerical experiences are shown to discuss the performance of the algorithm.

Keywords: Geometric inverse problem, Cauchy problem, Data completion problem, Shape optimization problem, Inverse obstacle problem, Laplace's equation, Kohn-Vogelius functional.

AMS Classification: 35R30, 49Q10, 35N25, 35R25

## 1 Introduction and problem setting

**The inverse obstacle problem with partial Cauchy data.** In this work we deal with the inverse problem of obstacle detection defined as follows. Let  $\Omega$  be a bounded connected Lipschitz open set of  $\mathbb{R}^d$  (with  $d = 2$  or  $d = 3$ ) with a boundary  $\partial\Omega$  divided into two components, the nonempty (relatively) open sets  $\Gamma_{obs}$  and  $\Gamma_i$ , such that  $\overline{\Gamma_{obs}} \cup \overline{\Gamma_i} = \partial\Omega$ . For some nontrivial data  $(g_N, g_D) \in H^{-1/2}(\Gamma_{obs}) \times H^{1/2}(\Gamma_{obs})$ , we consider the following obstacle problem:

---

\*Institut de Mathématiques de Toulouse, Université de Toulouse, F-31062 Toulouse Cedex 9, France.  
fabien.caubet@math.univ-toulouse.fr

†Institut de Mathématiques de Toulouse, Université de Toulouse, F-31062 Toulouse Cedex 9, France.  
jeremi.darde@math.univ-toulouse.fr

‡Centre for Biotechnology and Bioengineering - CeBiB, Universidad de Chile, Beauchef 851, Santiago, Chile & Institut de Mathématiques de Toulouse, Université de Toulouse, F-31062 Toulouse Cedex 9, France.  
matiasgodoy@uchile.cl

Find a set  $\omega^* \in \mathcal{D}$  and a solution  $u \in H^1(\Omega \setminus \overline{\omega^*}) \cap C^0(\overline{\Omega \setminus \omega^*})$   
of the following overdetermined boundary values problem:

$$\begin{cases} -\Delta u = 0 & \text{in } \Omega \setminus \overline{\omega^*} \\ u = g_D & \text{on } \Gamma_{obs} \\ \partial_\nu u = g_N & \text{on } \Gamma_{obs} \\ u = 0 & \text{on } \omega^*. \end{cases} \quad (1.1)$$

Here

$$\mathcal{D} := \left\{ \omega \subset\subset \Omega : \omega \text{ is a simply connected open set, } \partial\omega \text{ is of class } W^{2,\infty}, \right. \\ \left. d(x, \partial\Omega) > d_0 \text{ for all } x \in \omega, \Omega \setminus \overline{\omega} \text{ is connected} \right\}, \quad (1.2)$$

with  $d_0$  a fixed (small) parameter. In other words, the problem is to reconstruct an inclusion  $\omega^*$  characterized by a Dirichlet condition from the knowledge of some data  $(g_N, g_D)$  on the accessible part  $\Gamma_{obs}$  of the frontier of the domain of study, *no data at all being provided on the inaccessible part of the boundary*  $\Gamma_i$  (see Figure 1 for an illustration of the notations).

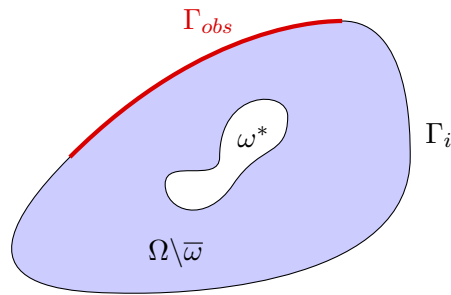


Figure 1: A possible configuration for the obstacle problem.

It is known for a long time now that Problem (1.1) admits at most one solution, as claimed by the following *identifiability result*<sup>1</sup> (see for example [15, Theorem 1.1], [24, Theorem 5.1] or [26, Proposition 4.4, page 87]):

**Theorem 1.1.** *The domain  $\omega$  and the function  $u$  that satisfy (1.1) are uniquely defined by the nontrivial Cauchy data  $(g_N, g_D)$ .*

It is also well-known that Problem (1.1) is severely ill-posed: the problem may fail to have a solution and, even when a solution exists, the problem is highly unstable. More precisely, the best one can expect is a logarithmic stability for problem (1.1) (see e.g. [4, 28]). In this work we focus on the reconstruction problem: our aim is to propose and test a numerical method to reconstruct (an approximation of )  $\omega^*$  from the (possibly noisy) data  $(g_N, g_D)$ .

Numerous methods have been proposed to solve this problem : sampling methods [43], methods based on conformal mappings [35], on integral equations [40, 44], level-set method coupled with quasi-reversibility in the exterior approach [15], among others. Among all of them, shape optimization methods (see e.g. [3, 18, 32]) present interesting features: in particular, they are easily adaptable to problem governed by a different partial differential equation, such as Stokes system (see e.g. [5, 20, 22, 33]), and obstacle characterized

<sup>1</sup>Actually, Theorem 1.1 is true only assuming that  $\omega^*$  has a continuous boundary (see [15, Theorem 1.1]).

by different limit conditions, such as Neumann or generalized boundary conditions (see e.g. [8, 21]). However, since such methods rely on the minimization of a (shape) cost-type functional which in turn needs the resolution of several well-posed direct problems, they need in particular some boundary data *on the whole boundary of the domain of study*, and therefore cannot be directly used for Problem (1.1).

**Remark 1.2.** *To the best of our knowledge, among all the methods cited above, only the exterior approach deals with the inverse obstacle problem with partial Cauchy data. However, the exterior approach has been specifically developed to deal with obstacles characterized by a Dirichlet-type boundary condition, and its adaptation to a Neumann-type condition is still an open question.*

*One aim of the method presented in this paper is to overcome this boundary conditions limitation. Indeed, the proposed method could be naturally adapted to Neumann boundary conditions for example and is then an effective alternative method to deal with partial Cauchy data.*

Our main objective is to adapt shape optimization methods for the inverse obstacle problem to the case where data are not available on the whole boundary of the domain of study. To do so, our strategy is to solve the inverse obstacle problem and a *data completion problem* in order to reconstruct the obstacle and the missing data at once. We do so through the minimization of a *Kohn-Vogelius* functional, which will have both the shape of  $\omega^*$  and the unknown data as variable, since such type of functional has already been used successfully to solve obstacle problems and data completion problem separately (see e.g. [6, 3]).

**The data completion problem.** Let us assume for a while that the obstacle  $\omega^*$  is known. The data completion problem consists in recovering data on the whole boundary, specifically on the inaccessible part  $\Gamma_i$ , from the overdetermined data  $(g_N, g_D)$  on  $\Gamma_{obs}$ , that is:

$$\begin{aligned} & \text{find } u \in \mathbf{H}^1(\Omega \setminus \overline{\omega^*}, \Delta) \text{ such that} \\ & \left\{ \begin{array}{ll} -\Delta u = 0 & \text{in } \Omega \setminus \overline{\omega^*} \\ u = g_D & \text{on } \Gamma_{obs} \\ \partial_\nu u = g_N & \text{on } \Gamma_{obs} \\ u = 0 & \text{on } \partial\omega^*. \end{array} \right. \end{aligned} \quad (1.3)$$

The data completion problem is known to be severely ill-posed, see for example [9] where the exponential ill-posedness is clearly highlighted. In particular, it has at most one solution but it may have no solution and, when a solution exists, it does not depend continuously on the given data (and therefore the same is true for the missing data); the well-known example of Hadamard [34] is an example of this behavior.

**Definition 1.3.** *A pair  $(g_N, g_D) \in \mathbf{H}^{-1/2}(\Gamma_{obs}) \times \mathbf{H}^{1/2}(\Gamma_{obs})$  will be called **compatible** if there exists (a necessarily unique)  $u \in \mathbf{H}^1(\Omega \setminus \overline{\omega^*}, \Delta)$  harmonic such that  $u|_{\Gamma_{obs}} = g_D$  and  $\partial_\nu u|_{\Gamma_{obs}} = g_N$ .*

If a given pair  $(g_N, g_D)$  is not compatible, we may approximate it by a sequence of compatible data, as the following result asserts (see Fursikov [30, Chapter 3] or Andrieux [6]):

**Lemma 1.4.** *We have the two following density results.*

1. *For a fixed  $g_D \in \mathbf{H}^{1/2}(\Gamma_{obs})$ , the set of data  $g_N$  for which there exists a function  $u \in \mathbf{H}^1(\Omega \setminus \overline{\omega^*}, \Delta)$  satisfying the Cauchy problem (1.3) is dense in  $\mathbf{H}^{-1/2}(\Gamma_{obs})$ .*

2. For a fixed  $g_N \in \mathbf{H}^{-1/2}(\Gamma_{obs})$ , the set of data  $g_D$  for which there exists a function  $u \in \mathbf{H}^1(\Omega \setminus \bar{\omega}^*, \Delta)$  satisfying the Cauchy problem (1.3) is dense in  $\mathbf{H}^{1/2}(\Gamma_{obs})$ .

Due to the ill-posedness, regularization techniques are mandatory to solve the problem numerically. Several approaches have been proposed: among others, we recall the work of Cimetière *et al.* [23] who consider a fixed point scheme for an appropriate operator. In [10, 7, 11], Ben Belgacem *et al.* propose a complete study of the problem based on the Steklov-Poincaré operator and a Lavrentiev regularization. We also mention the works of Bourgeois *et al.* [13, 14] based on the quasi-reversibility method and a generalization to a wider family of systems is presented by Dardé in [27]. Burman in [19] proposes a regularization through discretization : in particular, he obtains an optimal convergence result of the discretized solution to the exact one. In the particular case of a 2d problem, Leblond *et al.* in [41] use a complex-analytic approach to recover the solution of the Cauchy problem respecting furthermore additional pointwise constraints in the domain. Let us also mention the work of Kozlov *et al.* [39] which presents the classical KMF algorithm used widely for numerical simulations. Several works consider modifications of the KMF algorithm in order to improve their speed of convergence as the work of Abouchabaka *et al.* [1]. The work of Andrieux *et al.* [6] presents another approach considering the minimization of an energy-like functional and presents an algorithm which is equivalent to the KMF algorithm formulation. The work of Aboulaich *et al.* [2] considers a control type method for the numerical resolution of the Cauchy problem for Stokes system and, as an example of regularization techniques employed in this problem, we mention the work of Han *et al.* [36] in which a regularization of an energy functional is considered for an annular domain.

In this work, we follow the idea developed for example in [10, 7, 11, 6]: we study the data completion problem through the minimization of a Kohn-Vogelius type cost functional which admits the solution of Problem (1.3) as minimizer, if such a solution exists. In order to deal with the ill-posedness previously mentioned, we consider a Tikhonov regularization of the functional which ensures the existence of a minimizer even for not compatible data thanks to the gained of coerciveness and, in case of compatible data, the convergence towards the exact solution. In case of noisy data, we propose a strategy to choose the regularization parameter in order to preserve convergence to the unpolluted solution.

**The Kohn-Vogelius functional.** As mentioned, the two previous problems, that is the inverse obstacle problem and the data completion problem, can be studied through the minimization of a cost functional. Thus our idea is to define a well-appropriated Kohn-Vogelius functional, which depends both on the shape  $\omega$  and on the missing data on  $\Gamma_i$ , to solve Problem (1.1).

More precisely, we focus on the following optimization problem:

$$(\omega^*, \varphi^*, \psi^*) \in \underset{(\omega, \varphi, \psi) \in \mathcal{D} \times \mathbf{H}^{-1/2}(\Gamma_i) \times \mathbf{H}^{1/2}(\Gamma_i)}{\operatorname{argmin}} \mathcal{K}(\omega, \varphi, \psi) \quad (1.4)$$

where  $\mathcal{K}$  is the nonnegative Kohn-Vogelius cost functional defined by

$$\mathcal{K}(\omega, \varphi, \psi) = \frac{1}{2} \int_{\Omega \setminus \bar{\omega}} |\nabla u_\varphi^{g_D}(\omega) - \nabla u_\psi^{g_N}(\omega)|^2, \quad (1.5)$$

where  $u_\varphi^{g_D}(\omega) \in \mathbf{H}^1(\Omega \setminus \bar{\omega})$  and  $u_\psi^{g_N}(\omega) \in \mathbf{H}^1(\Omega \setminus \bar{\omega})$  are the respective solutions of the fol-

lowing problems

$$\left\{ \begin{array}{ll} -\Delta u_\varphi^{g_D}(\omega) = 0 & \text{in } \Omega \setminus \bar{\omega} \\ u_\varphi^{g_D}(\omega) = g_D & \text{on } \Gamma_{obs} \\ \partial_\nu u_\varphi^{g_D}(\omega) = \varphi & \text{on } \Gamma_i \\ u_\varphi^{g_D}(\omega) = 0 & \text{on } \partial\omega \end{array} \right. \quad \text{and} \quad \left\{ \begin{array}{ll} -\Delta u_\psi^{g_N}(\omega) = 0 & \text{in } \Omega \setminus \bar{\omega} \\ \partial_\nu u_\psi^{g_N}(\omega) = g_N & \text{on } \Gamma_{obs} \\ u_\psi^{g_N}(\omega) = \psi & \text{on } \Gamma_i \\ u_\psi^{g_N}(\omega) = 0 & \text{on } \partial\omega. \end{array} \right. \quad (1.6)$$

If the inverse problem (1.1) has a solution, then the identifiability result 1.1 ensures that  $\mathcal{K}(\omega, \varphi, \psi) = 0$  if and only if  $(\omega, \varphi, \psi) = (\omega^*, \varphi^*, \psi^*)$  (and in this case  $u_{\varphi^*}^{g_D} = u_{\psi^*}^{g_N} = u$  where  $u$  is the solution of the Cauchy problem in  $\Omega \setminus \bar{\omega}^*$ ).

In the rest of the paper, to simplify notations, we denote  $u_\varphi^{g_D}(\omega)$  and  $u_\psi^{g_N}(\omega)$  by respectively  $u_\varphi$  and  $u_\psi$ , and only precise the dependance with respect to  $g_D$  and  $g_N$  when it is necessary. Moreover we introduce the functions  $v_\varphi := u_\varphi^0$  and  $v_\psi := u_\psi^0$  (which also depend on  $\omega$ ) which play an important role in the following study. We precise that they satisfy respectively

$$\left\{ \begin{array}{ll} -\Delta v_\varphi = 0 & \text{in } \Omega \setminus \bar{\omega} \\ v_\varphi = 0 & \text{on } \Gamma_{obs} \\ \partial_\nu v_\varphi = \varphi & \text{on } \Gamma_i \\ v_\varphi = 0 & \text{on } \partial\omega \end{array} \right. \quad \text{and} \quad \left\{ \begin{array}{ll} -\Delta v_\psi = 0 & \text{in } \Omega \setminus \bar{\omega} \\ \partial_\nu v_\psi = 0 & \text{on } \Gamma_{obs} \\ v_\psi = \psi & \text{on } \Gamma_i \\ v_\psi = 0 & \text{on } \partial\omega. \end{array} \right. \quad (1.7)$$

**Remark 1.5.** *Note that the two problems appearing in (1.6) are well-posed for any  $(\varphi, \psi) \in H^{-1/2}(\Gamma_i) \times H^{1/2}(\Gamma_i)$ , without additional compatibility conditions between  $g_D$  and  $\varphi$  for the first problem and between  $g_N$  and  $\psi$  for the second. This is of particular interest for numerical implementations, as the considered setting allows to consider the classical Sobolev spaces and therefore the implementations can be done with classical finite element method softwares without any additional adjustments. The same remark obviously holds for the problems appearing in (1.7).*

Then we propose a method in order to solve the obstacle problem with partial boundary data. The use of a regularized extended functional is suggested in order to deal with the ill-posedness of the data completion part. We implement a gradient algorithm which uses the derivatives of  $\mathcal{K}$  with respect to the unknown boundary data and with respect to the shape in order to reconstruct the unknown obstacle only from partial boundary measurements. The main novelty of this work is composed in first place by providing a method in order to solve numerically the obstacle problem with partial boundary data by means of an *easy-to-implement* strategy in order to solve this problem. The division in two well-posed problems allows to implement an algorithm with any finite element library (such as FreeFEM++ [37] for example) and the consideration of a Kohn-Vogelius approach allows to implement optimization tools such as gradient methods. On the other hand, we have proposed a *natural* strategy to solve the data completion problem, presenting a rigorous analysis regularizing the associated functional via a Tikhonov regularization, which allows to deal with corrupted data.

**Organization of the paper** The paper is organized as follows. First, we introduce below the adopted notations. Then, in Section 2, we study the data completion problem as the minimization of an energy-like error/cost functional. To deal with noisy data, we propose and study a regularized version of the functional, considering in particular the problem of choosing the parameter of regularization with respect to a priori knowledge on the noise amplitude (see Subsection 2.3). Finally, in Section 3, we come back to the

inverse obstacle problem using the previously analyzed data completion problem and using geometrical shape optimization methods. We then propose an algorithm and provides several numerical examples of reconstruction.

**Introduction of the general notations.** For a bounded open set  $\Omega$  of  $\mathbb{R}^d$  ( $d \in \mathbb{N}^*$ ) with a (piecewise) Lipschitz boundary  $\partial\Omega$ , we precise that the notation  $\int_{\Omega} u$  means  $\int_{\Omega} u(x)dx$  which is the classical Lebesgue integral. Moreover, we use the notation  $\int_{\partial\Omega} u$  to denote the boundary integral  $\int_{\partial\Omega} u(x)ds(x)$ , where  $ds$  represents the surface Lebesgue measure on the boundary. We also introduce the exterior unit normal  $\nu$  of the domain  $\Omega$  and  $\partial_{\nu}u$  will denote the normal derivative of  $u$ .

For  $s \geq 0$  we denote by  $L^2(\Omega)$ ,  $L^2(\partial\Omega)$ ,  $H^s(\Omega)$ ,  $H^s(\partial\Omega)$ ,  $H_0^s(\Omega)$ , the usual Lebesgue and Sobolev spaces of scalar functions in  $\Omega$  or on  $\partial\Omega$ . The classical scalar product, norm and semi-norm on  $H^s(\Omega)$  are respectively denoted by  $(\cdot, \cdot)_{H^s(\Omega)}$ ,  $\|\cdot\|_{H^s(\Omega)}$  and  $|\cdot|_{H^s(\Omega)}$ . Moreover, we introduce the space  $H^1(\Omega, \Delta)$  given by

$$H^1(\Omega, \Delta) := \{u \in H^1(\Omega) : \Delta u \in L^2(\Omega)\}.$$

This space endowed with the scalar product

$$(u, v)_{H^1(\Omega, \Delta)} := (u, v)_{H^1(\Omega)} + (\Delta u, \Delta v)_{L^2(\Omega)}$$

is an Hilbert space, and each element of this space admits a normal derivative on  $\partial\Omega$  which belongs to  $H^{-1/2}(\partial\Omega)$ . In particular, for each  $u \in H^1(\Omega, \Delta)$  and  $v \in H^1(\Omega)$ , the well-known Green formula is valid:

$$\int_{\Omega} (\Delta u v + \nabla u \cdot \nabla v) dx = \left\langle \frac{\partial u}{\partial n}, v \right\rangle_{-1/2, 1/2, \partial\Omega}.$$

## 2 On the data completion problem

In this section we prove some theoretical results concerning the data completion problem, that is the case where the object is known. Then, in order to simplify the notations, we will consider here the case  $\omega = \emptyset$  but all the presented results can be easily adapted to the case  $\omega \neq \emptyset$ . Hence, the previous Kohn-Vogelius functional (1.5) is now defined, for  $(\varphi, \psi) \in H^{-1/2}(\Gamma_i) \times H^{1/2}(\Gamma_i)$ , by

$$\mathcal{K}(\varphi, \psi) = \frac{1}{2} \int_{\Omega} |\nabla u_{\varphi} - \nabla u_{\psi}|^2 \quad (2.1)$$

and the previous problems (1.6) and (1.7) become

$$\begin{cases} -\Delta u_{\varphi} = 0 & \text{in } \Omega \\ u_{\varphi} = g_D & \text{on } \Gamma_{obs} \\ \partial_{\nu} u_{\varphi} = \varphi & \text{on } \Gamma_i \end{cases} \quad \text{and} \quad \begin{cases} -\Delta u_{\psi} = 0 & \text{in } \Omega \\ \partial_{\nu} u_{\psi} = g_N & \text{on } \Gamma_{obs} \\ u_{\psi} = \psi & \text{on } \Gamma_i, \end{cases} \quad (2.2)$$

and

$$\begin{cases} -\Delta v_{\varphi} = 0 & \text{in } \Omega \setminus \bar{\omega} \\ v_{\varphi} = 0 & \text{on } \Gamma_{obs} \\ \partial_{\nu} v_{\varphi} = \varphi & \text{on } \Gamma_i \end{cases} \quad \text{and} \quad \begin{cases} -\Delta v_{\psi} = 0 & \text{in } \Omega \setminus \bar{\omega} \\ \partial_{\nu} v_{\psi} = 0 & \text{on } \Gamma_{obs} \\ v_{\psi} = \psi & \text{on } \Gamma_i, \end{cases} \quad (2.3)$$

where  $(g_N, g_D) \in H^{-1/2}(\Gamma_{obs}) \times H^{1/2}(\Gamma_{obs})$  is a given Cauchy pair which may be compatible or not (see Definition 1.3).

**Remark 2.1.** We can notice that (assuming enough regularity, if not we obtain a similar expression with duality products), after integration by parts, we get:

$$\mathcal{K}(\varphi, \psi) = \frac{1}{2} \int_{\Gamma_{obs}} (\partial_\nu u_\varphi - g_N)(g_D - u_\psi) + \frac{1}{2} \int_{\Gamma_i} (\varphi - \partial_\nu u_\psi)(u_\varphi - \psi).$$

This expression shows that the cost functional  $\mathcal{K}$  measures the error between  $u_\varphi$  and  $u_\psi$  as integrals only involving the boundary of the domain  $\Omega$ .

## 2.1 The Kohn-Vogelius functional

We first explore the properties of the Kohn-Vogelius functional  $\mathcal{K}$  given by (2.1).

**Proposition 2.2.** *The functional  $\mathcal{K}$  satisfies the following properties.*

1.  $\mathcal{K}$  is continuous, convex, positive and its infimum is zero.
2. When  $\mathcal{K}(\varphi, \psi)$  reaches its minimum with  $(\varphi^*, \psi^*) = \operatorname{argmin}_{(\varphi, \psi)} \mathcal{K}(\varphi, \psi)$  we have  $u_{\varphi^*} = u_{\psi^*} + C = u_{\psi^* + C}$  where  $C$  is any constant in  $\mathbb{R}$ . Therefore  $(\varphi^*, \psi^* + C)$  is also a minimizer of  $\mathcal{K}$ . Moreover, in this case,  $u_{\varphi^*}$  solves the Cauchy problem.
3. If we restrict  $\mathcal{K}$  to the space  $\mathbf{H}^{-1/2}(\Gamma_i) \times \mathbf{H}^{1/2}(\Gamma_i) / \mathbb{R}$  then a minimizer of  $\mathcal{K}$  is unique.
4. The first order optimality condition for  $(\varphi^*, \psi^*) \in \mathbf{H}^{-1/2}(\Gamma_i) \times \mathbf{H}^{1/2}(\Gamma_i)$  to be a minimizer is, for all  $(\tilde{\varphi}, \tilde{\psi}) \in \mathbf{H}^{-1/2}(\Gamma_i) \times \mathbf{H}^{1/2}(\Gamma_i)$ ,

$$\int_{\Omega} \nabla(v_{\varphi^*} - v_{\psi^*}) \cdot \nabla(v_{\tilde{\varphi}} - v_{\tilde{\psi}}) = \int_{\Omega} \left( \nabla u_0^{g_D} \cdot \nabla v_{\tilde{\psi}} + \nabla u_0^{g_N} \cdot \nabla v_{\tilde{\varphi}} \right). \quad (2.4)$$

*Proof.* We prove each statement.

1. Continuity, convexity and positiveness are obvious. To prove that  $\inf_{(\varphi, \psi)} \mathcal{K}(\varphi, \psi) = 0$ , we have to consider two cases. If the pair  $(g_N, g_D)$  is compatible, we consider  $\varphi^* := \partial_\nu u_{ex}|_{\Gamma_i}$  and  $\psi^* := u_{ex}|_{\Gamma_i}$  and then obtain  $\mathcal{K}(\varphi^*, \psi^*) = 0$ . Let us now focus on the non-compatible case. Thanks to the density lemma 1.4, we can approximate  $g_D$  by a sequence  $(g_D^n)_n$  in a way that the pairs  $(g_N, g_D^n)_n$  are compatibles for all  $n \in \mathbb{N}$ . For each  $n$ , consider  $(\varphi_n^*, \psi_n^*)$  the minimizer of the Kohn-Vogelius function for the data  $(g_N, g_D^n)$  which implies that  $\nabla u_{\varphi_n^*}^{g_D^n} = \nabla u_{\psi_n^*}^{g_N}$ . Then we have

$$\begin{aligned} \mathcal{K}(\varphi_n^*, \psi_n^*) &= \frac{1}{2} \left| u_{\varphi_n^*}^{g_D^n} - u_{\psi_n^*}^{g_N} \right|_{\mathbf{H}^1(\Omega)}^2 = \frac{1}{2} \left| u_{\varphi_n^*}^{g_D} - u_{\varphi_n^*}^{g_D^n} \right|_{\mathbf{H}^1(\Omega)}^2 = \frac{1}{2} \left| u_0^{g_D - g_D^n} \right|_{\mathbf{H}^1(\Omega)}^2 \\ &\leq C \|g_D - g_D^n\|_{\mathbf{H}^{1/2}(\Gamma_i)}^2 \xrightarrow{n \rightarrow \infty} 0, \end{aligned}$$

which concludes the proof.

2. The first and second assertions are obvious from the definition of the functional  $\mathcal{K}$ . Moreover, since  $u_{\varphi^*}$  is equal to  $u_{\psi^*}$  up to a constant, it solves the Cauchy problem (1.3).
3. This comes from the definition of quotient space.
4. Standard computations give the result noticing that

$$\int_{\Omega} \nabla u_0^{g_D} \cdot \nabla v_{\tilde{\varphi}} = 0 \quad \text{and} \quad \int_{\Omega} \nabla u_0^{g_N} \cdot \nabla v_{\tilde{\psi}} = 0.$$



□

**Remark 2.3.** *Actually, point 2. is an “if and only if statement”, as if the Cauchy problem admits a solution  $u_{ex}$ , then  $\varphi_{ex} = \partial_\nu u_{ex}$  and  $\psi_{ex} = u_{ex}$  satisfy  $\mathcal{K}(\varphi_{ex}, \psi_{ex}) = 0$  and therefore minimize  $\mathcal{K}$ .*

Let us introduce the bilinear form  $a : (\mathbf{H}^{-1/2}(\Gamma_i) \times \mathbf{H}^{1/2}(\Gamma_i))^2 \rightarrow \mathbb{R}$  and the linear form  $\ell : \mathbf{H}^{-1/2}(\Gamma_i) \times \mathbf{H}^{1/2}(\Gamma_i) \rightarrow \mathbb{R}$  defined, for all  $(\varphi, \psi), (\tilde{\varphi}, \tilde{\psi}) \in \mathbf{H}^{-1/2}(\Gamma_i) \times \mathbf{H}^{1/2}(\Gamma_i)$ , by

$$\begin{aligned} a((\varphi, \psi), (\tilde{\varphi}, \tilde{\psi})) &:= \int_{\Omega} \nabla(v_\varphi - v_\psi) \cdot \nabla(v_{\tilde{\varphi}} - v_{\tilde{\psi}}) \\ \ell(\varphi, \psi) &:= \int_{\Omega} \nabla(u_0^{g_N} - u_0^{g_D}) \cdot \nabla(v_\varphi - v_\psi) = \int_{\Omega} (\nabla u_0^{g_D} \cdot \nabla v_\psi + \nabla u_0^{g_N} \cdot \nabla v_\varphi). \end{aligned} \quad (2.5)$$

Then the optimality condition (2.4) writes

$$a((\varphi^*, \psi^*), (\tilde{\varphi}, \tilde{\psi})) = \ell(\tilde{\varphi}, \tilde{\psi}), \quad \forall (\tilde{\varphi}, \tilde{\psi}) \in \mathbf{H}^{-1/2}(\Gamma_i) \times \mathbf{H}^{1/2}(\Gamma_i). \quad (2.6)$$

By the fact that  $\mathcal{K}$  is not coercive, we cannot assume that  $\mathcal{K}$  reaches its minimum in general. The following proposition states a condition for minimizing sequences in order to assure the existence of minimizers for the functional and, at the same time, a solution of our inverse problem.

**Proposition 2.4.** *Let  $(\varphi_n^*, \psi_n^*)_n \subset \mathbf{H}^{-1/2}(\Gamma_i) \times \mathbf{H}^{1/2}(\Gamma_i)$  a minimizing sequence of  $\mathcal{K}$ .  $(\varphi_n^*, \psi_n^*)_n$  is bounded if and only if the Cauchy problem (1.3) admits a solution  $u_{ex}$ . In this case we have  $u_{\varphi_n^*} \rightharpoonup u_{ex}$  weakly in  $\mathbf{H}^1(\Omega)$  and all the minimizing sequences of  $\mathcal{K}$  are bounded.*

*Proof.* Consider the sequence  $(\varphi_n^*, \psi_n^*)_n$  bounded in  $\mathbf{H}^{-1/2}(\Gamma_i) \times \mathbf{H}^{1/2}(\Gamma_i)$ . Then there exists  $(\varphi^*, \psi^*) \in \mathbf{H}^{-1/2}(\Gamma_i) \times \mathbf{H}^{1/2}(\Gamma_i)$  such that, up to a subsequence, we have  $(\varphi_n^*, \psi_n^*) \rightharpoonup (\varphi^*, \psi^*)$  in  $\mathbf{H}^{-1/2}(\Gamma_i) \times \mathbf{H}^{1/2}(\Gamma_i)$ . As  $\mathcal{K}$  is convex and continuous in  $\mathbf{H}^{-1/2}(\Gamma_i) \times \mathbf{H}^{1/2}(\Gamma_i)$ , it is weakly lower semi-continuous. Then, since the sequence  $(\varphi_n^*, \psi_n^*)_n$  is a minimizing sequence of  $\mathcal{K}$ ,

$$\mathcal{K}(\varphi^*, \psi^*) \leq \liminf_k \mathcal{K}(\varphi_{n_k}^*, \psi_{n_k}^*) = \inf_{(\varphi, \psi)} \mathcal{K}(\varphi, \psi) = 0.$$

Hence  $\mathcal{K}(\varphi^*, \psi^*) = 0$ . This implies  $u_{\varphi^*} = u_{\psi^*} + C$  for some  $C \in \mathbb{R}$ . Then, since  $\partial_\nu u_{\varphi^*}|_{\Gamma_{obs}} = \partial_\nu u_{\psi^*}|_{\Gamma_{obs}} = g_N$ , the function  $u_{\varphi^*}$  satisfies

$$\begin{cases} -\Delta u_{\varphi^*} = 0 & \text{in } \Omega \\ u_{\varphi^*} = g_D & \text{on } \Gamma_{obs} \\ \partial_\nu u_{\varphi^*} = g_N & \text{on } \Gamma_{obs}. \end{cases}$$

Thus  $u_{\varphi^*} = u_{ex}$  is the solution of the Cauchy problem and  $u_{\psi^*} = u_{ex} + C$  for some  $C \in \mathbb{R}$ .

Now, in order to prove the weak convergence of  $u_{\varphi_n^*}$  to  $u_{ex}$ , note that boundedness of  $(\varphi_n^*, \psi_n^*)_n$  implies, due to well-posedness of the involved problems, the boundedness of the sequences  $(u_{\varphi_n^*})_n$  and  $(u_{\psi_n^*})_n$  in  $\mathbf{H}^1(\Omega)$ . Therefore there exist  $u_1, u_2 \in \mathbf{H}^1(\Omega)$  such that, up to a subsequence,  $(u_{\varphi_n^*})_n \rightharpoonup u_1$  and  $(u_{\psi_n^*})_n \rightharpoonup u_2$  weakly in  $\mathbf{H}^1(\Omega)$ . Finally, thanks to the weak-continuity of normal derivative and trace operators,  $u_1|_{\Gamma_{obs}} = g_D$  and  $\partial_\nu u_2|_{\Gamma_{obs}} = g_N$ , and, by the uniqueness of the weak limit,  $\partial_\nu u_1|_{\Gamma_i} = \varphi^*$  and  $u_2|_{\Gamma_i} = \psi^*$ . Therefore  $u_1 = u_{\varphi^*} = u_{ex}$  and  $u_2 = u_{\psi^*} = u_{ex} + C$  for some  $C \in \mathbb{R}$ .

The converse statement is immediate, as if the Cauchy problem admits a solution  $u_{ex}$ , then  $\mathcal{K}$  admits a minimizer (see Remark 2.3) and, as it is a strictly convex function, it is therefore necessary coercive, which implies in particular that all the minimizing sequences are bounded. □

## 2.2 Regularization of the Kohn-Vogelius functional

As mentioned above, when the data completion problem has no solution, the minimization problem for  $\mathcal{K}$  fails to have one. Additionally, as recalled in the introduction, the data completion problem is ill-posed in the sense that, in case of the existence of solution, there is not a continuous dependence on the given data.

In order to overcome these difficulties, we consider a *Tikhonov regularization* of the Kohn-Vogelius functional, which, roughly speaking, allows us to get coerciveness and a better behavior with respect to noisy data. There is an extensive literature related to this type of regularization: we recommend in particular the book of Engl *et al.* [29] which describes in detail and in full generality the considered regularization.

From now on, for  $\varepsilon > 0$ , we introduce the regularized Kohn-Vogelius functional  $\mathcal{K}_\varepsilon : \mathbf{H}^{-1/2}(\Gamma_i) \times \mathbf{H}^{1/2}(\Gamma_i) \rightarrow \mathbb{R}$  given by

$$\mathcal{K}_\varepsilon(\varphi, \psi) := \mathcal{K}(\varphi, \psi) + \frac{\varepsilon}{2} \left( \|v_\varphi\|_{\mathbf{H}^1(\Omega)}^2 + \|v_\psi\|_{\mathbf{H}^1(\Omega)}^2 \right) = \mathcal{K}(\varphi, \psi) + \frac{\varepsilon}{2} \|(v_\varphi, v_\psi)\|_{(\mathbf{H}^1(\Omega))^2}^2, \quad (2.7)$$

where  $\mathcal{K}$  is the previous Kohn-Vogelius functional given by (2.1).  $\mathcal{K}_\varepsilon$  is a regularization of the standard  $\mathcal{K}$  functional, as it *always* admits a minimizer, regardless of the compatibility of the Cauchy data:

**Proposition 2.5.** *Given  $\varepsilon > 0$ , the functional  $\mathcal{K}_\varepsilon$  satisfies the following properties.*

1.  $\mathcal{K}_\varepsilon(\varphi, \psi)$  is continuous, strictly convex and coercive in  $\mathbf{H}^{-1/2}(\Gamma_i) \times \mathbf{H}^{1/2}(\Gamma_i)$ . Therefore there exists

$$(\varphi_\varepsilon^*, \psi_\varepsilon^*) := \underset{(\varphi, \psi)}{\operatorname{argmin}} \mathcal{K}_\varepsilon(\varphi, \psi).$$

2. The optimality condition for  $(\varphi_\varepsilon^*, \psi_\varepsilon^*)$  to be a minimizer of  $\mathcal{K}_\varepsilon$  is: for all  $(\tilde{\varphi}, \tilde{\psi}) \in \mathbf{H}^{-1/2}(\Gamma_i) \times \mathbf{H}^{1/2}(\Gamma_i)$ ,

$$a((\varphi_\varepsilon^*, \psi_\varepsilon^*), (\tilde{\varphi}, \tilde{\psi})) + \varepsilon \cdot b((\varphi_\varepsilon^*, \psi_\varepsilon^*), (\tilde{\varphi}, \tilde{\psi})) = \ell(\tilde{\varphi}, \tilde{\psi}) \quad (2.8)$$

where  $a(\cdot, \cdot)$  and  $\ell(\cdot)$  are previously defined by (2.5) and  $b(\cdot, \cdot)$  is defined for all  $(\varphi, \psi), (\tilde{\varphi}, \tilde{\psi}) \in \mathbf{H}^{-1/2}(\Gamma_i) \times \mathbf{H}^{1/2}(\Gamma_i)$  by

$$b((\varphi, \psi), (\tilde{\varphi}, \tilde{\psi})) = ((v_\varphi, v_\psi), (v_{\tilde{\varphi}}, v_{\tilde{\psi}}))_{\mathbf{H}^1(\Omega) \times \mathbf{H}^1(\Omega)}. \quad (2.9)$$

3. The bilinear form  $b$  defines an inner product on  $\mathbf{H}^{-1/2}(\Gamma_i) \times \mathbf{H}^{1/2}(\Gamma_i)$  and the associated norm  $\|\cdot\|_b$  is equivalent to the standard one in that space.

*Proof.* We prove each statement.

1. The continuity and convexity are obvious. Assume that  $\mathcal{K}_\varepsilon$  is not coercive. Then there exists a sequence  $(\varphi_n, \psi_n)_n$  and a constant  $C > 0$  such that

$$\lim_{n \rightarrow \infty} \|(\varphi_n, \psi_n)\|_{\mathbf{H}^{-1/2}(\Gamma_i) \times \mathbf{H}^{1/2}(\Gamma_i)} = +\infty \quad \text{and} \quad \mathcal{K}_\varepsilon(\varphi_n, \psi_n) < C.$$

This implies  $\|v_{\varphi_n}\|_{\mathbf{H}^1(\Omega)} < C$  and  $\|v_{\psi_n}\|_{\mathbf{H}^1(\Omega)} < C$  for all  $n$  which, by the continuity of trace and normal derivative operators, implies  $\|(\varphi_n, \psi_n)\|_{\mathbf{H}^{-1/2}(\Gamma_i) \times \mathbf{H}^{1/2}(\Gamma_i)} < C$  which is in contradiction with the original assumption.

The existence of minimizers comes from the continuity, convexity and coerciveness of  $\mathcal{K}_\varepsilon$  (see, e.g., [16, Chapter 3]).

2. As in the proof of Proposition 2.2, the result comes from a standard computation.
3. The fact that  $b$  defines an inner product is immediate from its bilinearity and the well-posedness of the problems solved by  $v_\varphi$  and  $v_\psi$ . The equivalence of norms comes from the continuity of the trace and normal derivative operators and the well-posedness of the problems solved by  $v_\varphi$  and  $v_\psi$ .

□

In the following, for  $\varepsilon > 0$ , we use the following notation (introduced in the previous proposition)

$$(\varphi_\varepsilon^*, \psi_\varepsilon^*) := \underset{(\varphi, \psi) \in \mathbf{H}^{-1/2}(\Gamma_i) \times \mathbf{H}^{1/2}(\Gamma_i)}{\operatorname{argmin}} \mathcal{K}_\varepsilon(\varphi, \psi)$$

which always exists due to Proposition 2.5. The following theorem relates the set of minimizers  $(\varphi_\varepsilon^*, \psi_\varepsilon^*)$  of  $\mathcal{K}_\varepsilon$  with the functional  $\mathcal{K}$  and states a condition to assure the existence of solution for the Cauchy problem (1.3).

**Theorem 2.6.** *The sequence  $(\varphi_\varepsilon^*, \psi_\varepsilon^*)_\varepsilon$  ( $\varepsilon \rightarrow 0$ ) is a minimizing sequence of  $\mathcal{K}$ . Therefore, it is a bounded sequence if and only if the Cauchy problem has a (necessarily unique) solution  $u_{ex}$ . In that case*

1.  $(\varphi_\varepsilon^*, \psi_\varepsilon^*)$  converges when  $\varepsilon$  goes to 0 to  $(\varphi^*, \psi^*)$ , a minimizer of  $\mathcal{K}$ , strongly in  $\mathbf{H}^{-1/2}(\Gamma_i) \times \mathbf{H}^{1/2}(\Gamma_i)$ ;
2.  $u_{\varphi_\varepsilon^*}$  converges strongly in  $\mathbf{H}^1(\Omega)$  to the solution  $u_{ex}$  of the Cauchy problem (1.3) when  $\varepsilon \rightarrow 0$ .

*Proof.* For all  $\varepsilon > 0$ , by definition of  $(\varphi_\varepsilon^*, \psi_\varepsilon^*) = \underset{(\varphi, \psi)}{\operatorname{argmin}} \mathcal{K}_\varepsilon(\varphi, \psi)$ ,

$$0 \leq \mathcal{K}(\varphi_\varepsilon^*, \psi_\varepsilon^*) \leq \mathcal{K}_\varepsilon(\varphi_\varepsilon^*, \psi_\varepsilon^*) \leq \mathcal{K}_\varepsilon(\varphi, \psi), \quad \forall (\varphi, \psi) \in \mathbf{H}^{-1/2}(\Gamma_i) \times \mathbf{H}^{1/2}(\Gamma_i).$$

Moreover, by definition of infimum, for  $\eta > 0$ , there exists  $(\varphi_\eta, \psi_\eta) \in \mathbf{H}^{-1/2}(\Gamma_i) \times \mathbf{H}^{1/2}(\Gamma_i)$  such that  $\mathcal{K}(\varphi_\eta, \psi_\eta) \leq \frac{\eta}{2}$ . Inserting this pair in the first inequality, we obtain

$$0 \leq \mathcal{K}(\varphi_\varepsilon^*, \psi_\varepsilon^*) \leq \mathcal{K}_\varepsilon(\varphi_\varepsilon^*, \psi_\varepsilon^*) \leq \mathcal{K}_\varepsilon(\varphi_\eta, \psi_\eta) \leq \frac{\varepsilon}{2} \|(v_{\varphi_\eta}, v_{\psi_\eta})\|_{\mathbf{H}^1(\Omega) \times \mathbf{H}^1(\Omega)}^2 + \frac{\eta}{2}.$$

Taking  $\varepsilon^* > 0$  sufficiently small such that  $\frac{\varepsilon}{2} \|(v_{\varphi_\eta}, v_{\psi_\eta})\|_{\mathbf{H}^1(\Omega) \times \mathbf{H}^1(\Omega)}^2 \leq \frac{\eta}{2}$  for all  $\varepsilon \in (0, \varepsilon^*)$ , we have

$$0 \leq \mathcal{K}(\varphi_\varepsilon^*, \psi_\varepsilon^*) \leq \mathcal{K}_\varepsilon(\varphi_\varepsilon^*, \psi_\varepsilon^*) \leq \eta, \quad \forall \varepsilon \in (0, \varepsilon^*).$$

Hence  $\mathcal{K}(\varphi_\varepsilon^*, \psi_\varepsilon^*) \xrightarrow{\varepsilon \rightarrow 0} 0$  (and  $\mathcal{K}_\varepsilon(\varphi_\varepsilon^*, \psi_\varepsilon^*) \xrightarrow{\varepsilon \rightarrow 0} 0$ ). Proposition 2.4 implies then that  $(\varphi_\varepsilon^*, \psi_\varepsilon^*)_\varepsilon$  is a bounded sequence if and only if the Cauchy problem admits a solution  $u_{ex}$ .

The same Proposition gives the following weak convergences:  $(\varphi_{\varepsilon_n}^*, \psi_{\varepsilon_n}^*) \rightharpoonup (\varphi^*, \psi^*)$  weakly in  $\mathbf{H}^{-1/2}(\Gamma_i) \times \mathbf{H}^{1/2}(\Gamma_i)$  and  $(u_{\varphi_{\varepsilon_n}^*}, u_{\psi_{\varepsilon_n}^*}) \rightharpoonup (u_{\varphi^*}, u_{\psi^*}) = (u_{ex}, u_{ex} + C)$  weakly in  $\mathbf{H}^1(\Omega) \times \mathbf{H}^1(\Omega)$ . In order to obtain strong convergence, notice that

$$0 \leq \frac{\varepsilon_n}{2} \|(\varphi_{\varepsilon_n}^*, \psi_{\varepsilon_n}^*)\|_b^2 \leq \mathcal{K}_{\varepsilon_n}(\varphi_{\varepsilon_n}^*, \psi_{\varepsilon_n}^*) \leq \mathcal{K}_{\varepsilon_n}(\varphi^*, \psi^*) = \frac{\varepsilon_n}{2} \|(\varphi^*, \psi^*)\|_b^2.$$

Then, passing to the lim sup,

$$\limsup_n \|(\varphi_{\varepsilon_n}^*, \psi_{\varepsilon_n}^*)\|_b \leq \|(\varphi^*, \psi^*)\|_b,$$

which proves the strong convergence for the data in  $\Gamma_i$ .

For the other strong convergence, it is enough to prove the strong convergence of  $v_{\varphi_{\varepsilon_n}^*}$  to  $v_{\varphi_{ex}} = v_{\varphi^*} = u_{\varphi^*} - u_0^{gD} = u_{ex} - u_0^{gD}$ . To this, notice that

$$\mathcal{K}_{\varepsilon_n}(\varphi_{\varepsilon_n}^*, \psi_{\varepsilon_n}^*) \leq \mathcal{K}_{\varepsilon_n}(\varphi_{ex}, \psi_{ex} + C) = \frac{\varepsilon_n}{2} \|(v_{\varphi_{ex}}, v_{\psi_{ex}+C})\|_{\mathbf{H}^1(\Omega) \times \mathbf{H}^1(\Omega)}^2.$$

Hence

$$\limsup_n \|(v_{\varphi_{\varepsilon_n}^*}, v_{\psi_{\varepsilon_n}^*})\|_{\mathbf{H}^1(\Omega) \times \mathbf{H}^1(\Omega)} \leq \|(v_{\varphi_{ex}}, v_{\psi_{ex}+C})\|_{\mathbf{H}^1(\Omega) \times \mathbf{H}^1(\Omega)},$$

which proves the strong convergence.  $\square$

**Remark 2.7.** We also have, for some  $C \in \mathbb{R}$ ,

$$u_{\psi_{\varepsilon}^*} \rightarrow u_{ex} + C \text{ in } \mathbf{H}^1(\Omega).$$

We now prove several properties which are useful in the next subsection where we define a regularizing parameter  $\varepsilon$  such that we can obtain convergence properties even then the data  $(g_N, g_D)$  is polluted with noise.

**Proposition 2.8.** Let  $(\varphi_{\varepsilon}^*, \psi_{\varepsilon}^*) \in \mathbf{H}^{-1/2}(\Gamma_i) \times \mathbf{H}^{1/2}(\Gamma_i)$  be the minimizer of  $\mathcal{K}_{\varepsilon}$ . We have the following statements.

1. The application  $F : \varepsilon \rightarrow (u_{\varphi_{\varepsilon}^*}, u_{\psi_{\varepsilon}^*}) \in \mathbf{H}^1(\Omega) \times \mathbf{H}^1(\Omega)$  is continuous for  $\varepsilon > 0$  and, if the data  $(g_N, g_D)$  is compatible, it could be continuously extended to 0 with  $F(0) = (u_{\varphi_{ex}}, u_{\psi_{ex}})$ .
2. The application  $F$  is (at least)  $\mathcal{C}^1((0, \infty), \mathbf{H}^1(\Omega) \times \mathbf{H}^1(\Omega))$ . Its derivative is given by  $F'(\varepsilon) = (v_{\varphi_{\varepsilon}'}', v_{\psi_{\varepsilon}'}')$  where the pair  $(\varphi_{\varepsilon}'', \psi_{\varepsilon}'')$   $\in \mathbf{H}^{-1/2}(\Gamma_i) \times \mathbf{H}^{1/2}(\Gamma_i)$  is the unique solution of

$$\begin{aligned} a((\varphi_{\varepsilon}'', \psi_{\varepsilon}''), (\varphi, \psi)) + \varepsilon b((\varphi_{\varepsilon}'', \psi_{\varepsilon}''), (\varphi, \psi)) &= -b((\varphi_{\varepsilon}, \psi_{\varepsilon}), (\varphi, \psi)), \\ \forall (\varphi, \psi) \in \mathbf{H}^{-1/2}(\Gamma_i) \times \mathbf{H}^{1/2}(\Gamma_i). \end{aligned} \quad (2.10)$$

3. The map  $\varepsilon \mapsto \frac{1}{2} |u_{\varphi_{\varepsilon}^*} - u_{\psi_{\varepsilon}^*}|_{\mathbf{H}^1(\Omega)}^2 \in \mathbb{R}$  is strictly increasing for  $\varepsilon > 0$ .

*Proof.* We prove each statement. We first recall that  $v_{\varphi}$  and  $v_{\psi}$  solve Problems (2.3).

1. Let  $h \in \mathbb{R}$  such that  $\varepsilon + h > 0$ . Let us prove that

$$\|u_{\varphi_{\varepsilon+h}^*} - u_{\varphi_{\varepsilon}^*}, u_{\psi_{\varepsilon+h}^*} - u_{\psi_{\varepsilon}^*}\|_{(\mathbf{H}^1(\Omega))^2} \xrightarrow{h \rightarrow 0} 0.$$

Then let us consider the optimal pairs  $(\varphi_{\varepsilon+h}^*, \psi_{\varepsilon+h}^*)$  and  $(\varphi_{\varepsilon}^*, \psi_{\varepsilon}^*)$ . Subtracting the optimality conditions of both pairs, we obtain, for all  $(\varphi, \psi) \in \mathbf{H}^{-1/2}(\Gamma_i) \times \mathbf{H}^{1/2}(\Gamma_i)$ ,

$$\begin{aligned} a((\varphi_{\varepsilon+h}^* - \varphi_{\varepsilon}^*, \psi_{\varepsilon+h}^* - \psi_{\varepsilon}^*), (\varphi, \psi)) + \varepsilon \cdot b((\varphi_{\varepsilon+h}^* - \varphi_{\varepsilon}^*, \psi_{\varepsilon+h}^* - \psi_{\varepsilon}^*), (\varphi, \psi)) \\ = -h \cdot b((\varphi_{\varepsilon+h}^* - \varphi_{\varepsilon}^*, \psi_{\varepsilon+h}^* - \psi_{\varepsilon}^*), (\varphi, \psi)). \end{aligned}$$

Choosing  $\varphi := \varphi_{\varepsilon+h}^* - \varphi_{\varepsilon}^*$  and  $\psi := \psi_{\varepsilon+h}^* - \psi_{\varepsilon}^*$ , we get

$$\begin{aligned} |v_{\varphi_{\varepsilon+h}^*} - v_{\varphi_{\varepsilon}^*} - (v_{\psi_{\varepsilon+h}^*} - v_{\psi_{\varepsilon}^*})|_{\mathbf{H}^1(\Omega)}^2 + \varepsilon \|(v_{\varphi_{\varepsilon+h}^*} - v_{\varphi_{\varepsilon}^*}, v_{\psi_{\varepsilon+h}^*} - v_{\psi_{\varepsilon}^*})\|_{(\mathbf{H}^1(\Omega))^2}^2 \\ = -h \cdot ((v_{\varphi_{\varepsilon+h}^*}, v_{\psi_{\varepsilon+h}^*}), (v_{\varphi_{\varepsilon+h}^* - \varphi_{\varepsilon}^*}, v_{\psi_{\varepsilon+h}^* - \psi_{\varepsilon}^*}))_{(\mathbf{H}^1(\Omega))^2}. \end{aligned}$$

Now, notice we have

$$\begin{aligned} & \|((v_{\varphi_{\varepsilon+h}^*}, v_{\psi_{\varepsilon+h}^*}), (v_{\varphi_{\varepsilon+h}^* - \varphi_{\varepsilon}^*}, v_{\psi_{\varepsilon+h}^* - \psi_{\varepsilon}^*}))\|_{(\mathbf{H}^1(\Omega))^2} \\ & \leq \| (v_{\varphi_{\varepsilon+h}^*}, v_{\psi_{\varepsilon+h}^*}) \|_{(\mathbf{H}^1(\Omega))^2} \| (v_{\varphi_{\varepsilon+h}^* - \varphi_{\varepsilon}^*}, v_{\psi_{\varepsilon+h}^* - \psi_{\varepsilon}^*}) \|_{(\mathbf{H}^1(\Omega))^2} \end{aligned}$$

which gives

$$\begin{aligned} & \| (v_{\varphi_{\varepsilon+h}^*} - v_{\varphi_{\varepsilon}^*}, v_{\psi_{\varepsilon+h}^*} - v_{\psi_{\varepsilon}^*}) \|_{(\mathbf{H}^1(\Omega))^2}^2 \\ & \leq \frac{|h|}{\varepsilon} \| (v_{\varphi_{\varepsilon+h}^*}, v_{\psi_{\varepsilon+h}^*}) \|_{(\mathbf{H}^1(\Omega))^2} \| (v_{\varphi_{\varepsilon+h}^*} - v_{\varphi_{\varepsilon}^*}, v_{\psi_{\varepsilon+h}^*} - v_{\psi_{\varepsilon}^*}) \|_{(\mathbf{H}^1(\Omega))^2} \end{aligned}$$

and then

$$\| (v_{\varphi_{\varepsilon+h}^*} - v_{\varphi_{\varepsilon}^*}, v_{\psi_{\varepsilon+h}^*} - v_{\psi_{\varepsilon}^*}) \|_{(\mathbf{H}^1(\Omega))^2} \leq \frac{|h|}{\varepsilon} \| (v_{\varphi_{\varepsilon+h}^*}, v_{\psi_{\varepsilon+h}^*}) \|_{(\mathbf{H}^1(\Omega))^2}.$$

Moreover, by definition of  $\mathcal{K}_{\varepsilon+h}$ ,

$$(\varepsilon + h) \| (v_{\varphi_{\varepsilon+h}^*}, v_{\psi_{\varepsilon+h}^*}) \|_{\mathbf{H}^1(\Omega)}^2 \leq \mathcal{K}_{\varepsilon+h}(\varphi_{\varepsilon+h}^*, \psi_{\varepsilon+h}^*) \leq \mathcal{K}_{\varepsilon+h}(0, 0).$$

Noticing that

$$\mathcal{K}_{\varepsilon+h}(0, 0) = \frac{1}{2} |u_0^{gD} - u_0^{gN}|_{\mathbf{H}^1(\Omega)}^2 \leq C \left( \|gD\|_{\mathbf{H}^{1/2}(\Gamma_{obs})}^2 + \|gN\|_{\mathbf{H}^{-1/2}(\Gamma_{obs})}^2 \right),$$

we obtain

$$\begin{aligned} & \| (v_{\varphi_{\varepsilon+h}^*} - v_{\varphi_{\varepsilon}^*}, v_{\psi_{\varepsilon+h}^*} - v_{\psi_{\varepsilon}^*}) \|_{(\mathbf{H}^1(\Omega))^2} \leq \frac{|h|}{\varepsilon} \| (v_{\varphi_{\varepsilon+h}^*}, v_{\psi_{\varepsilon+h}^*}) \|_{(\mathbf{H}^1(\Omega))^2} \\ & \leq \left( \|gD\|_{\mathbf{H}^{1/2}(\Gamma_{obs})}^2 + \|gN\|_{\mathbf{H}^{-1/2}(\Gamma_{obs})}^2 \right) \frac{|h|}{\varepsilon \sqrt{\varepsilon + h}} \xrightarrow{h \rightarrow 0} 0, \quad (2.11) \end{aligned}$$

which concludes the proof.

2. First, the existence and uniqueness of the solution  $(\varphi'_{\varepsilon}, \psi'_{\varepsilon}) \in \mathbf{H}^{-1/2}(\Gamma_i) \times \mathbf{H}^{1/2}(\Gamma_i)$  of Problem (2.10) is due to Lax-Milgram theorem. Indeed, the continuity of the bilinear form  $a(\cdot, \cdot) + \varepsilon b(\cdot, \cdot)$  and of the linear form  $-b((\varphi_{\varepsilon}^*, \psi_{\varepsilon}^*), (\cdot, \cdot))$  are due to the well-posedness of the problems solved by  $v_{\varphi}$  and  $v_{\psi}$  and the continuity of  $a(\cdot, \cdot) + \varepsilon b(\cdot, \cdot)$  is due to the continuity of trace operator and normal derivative operators.

Now, let us prove that the derivative of the function  $F$  is  $F'(\varepsilon) = (v_{\varphi'_{\varepsilon}}, v_{\psi'_{\varepsilon}})$ . For this, let  $h \in \mathbb{R}$  such that  $\varepsilon + h > 0$ . From the optimality conditions for  $(\varphi_{\varepsilon}^*, \psi_{\varepsilon}^*)$  and  $(\varphi_{\varepsilon+h}^*, \psi_{\varepsilon+h}^*)$  and the condition satisfied from  $(\varphi'_{\varepsilon}, \psi'_{\varepsilon})$ , we obtain

$$\begin{aligned} & a((\varphi_{\varepsilon+h}^* - \varphi_{\varepsilon}^* - h\varphi'_{\varepsilon}, \psi_{\varepsilon+h}^* - \psi_{\varepsilon}^* - h\psi'_{\varepsilon}), (\varphi, \psi)) \\ & \quad + \varepsilon \cdot b((\varphi_{\varepsilon+h}^* - \varphi_{\varepsilon}^* - h\varphi'_{\varepsilon}, \psi_{\varepsilon+h}^* - \psi_{\varepsilon}^* - h\psi'_{\varepsilon}), (\varphi, \psi)) \\ & \quad = h \cdot b((\varphi_{\varepsilon}^* - \varphi_{\varepsilon+h}^*, \psi_{\varepsilon}^* - \psi_{\varepsilon+h}^*), (\varphi, \psi)). \end{aligned}$$

Taking  $\varphi := \varphi_{\varepsilon+h}^* - \varphi_{\varepsilon}^* - h\varphi'_{\varepsilon}$  and  $\psi := \psi_{\varepsilon+h}^* - \psi_{\varepsilon}^* - h\psi'_{\varepsilon}$ , we use Hölder's inequality on the right side to get

$$\begin{aligned} & |u_{\varphi_{\varepsilon+h}^* - \varphi_{\varepsilon}^* - h\varphi'_{\varepsilon}} - u_{\psi_{\varepsilon+h}^* - \psi_{\varepsilon}^* - h\psi'_{\varepsilon}}|_{\mathbf{H}^1(\Omega)}^2 + \varepsilon \cdot \| (v_{\varphi_{\varepsilon+h}^* - \varphi_{\varepsilon}^* - h\varphi'_{\varepsilon}}, v_{\psi_{\varepsilon+h}^* - \psi_{\varepsilon}^* - h\psi'_{\varepsilon}}) \|_{(\mathbf{H}^1(\Omega))^2}^2 \\ & \leq |h| \| (v_{\varphi_{\varepsilon}^* - \varphi_{\varepsilon+h}^*}, v_{\psi_{\varepsilon}^* - \psi_{\varepsilon+h}^*}) \|_{(\mathbf{H}^1(\Omega))^2} \| (v_{\varphi_{\varepsilon+h}^* - \varphi_{\varepsilon}^* - h\varphi'_{\varepsilon}}, v_{\psi_{\varepsilon+h}^* - \psi_{\varepsilon}^* - h\psi'_{\varepsilon}}) \|_{(\mathbf{H}^1(\Omega))^2} \end{aligned}$$

and then,

$$\|v_{\varphi_{\varepsilon+h}^* - \varphi_{\varepsilon}^* - h\varphi'_{\varepsilon}}, v_{\psi_{\varepsilon+h}^* - \psi_{\varepsilon}^* - h\psi'_{\varepsilon}}\|_{(\mathbf{H}^1(\Omega))^2} \leq \frac{|h|}{\varepsilon} \|v_{\varphi_{\varepsilon}^* - \varphi_{\varepsilon+h}^*}, v_{\psi_{\varepsilon}^* - \psi_{\varepsilon+h}^*}\|_{(\mathbf{H}^1(\Omega))^2}.$$

Hence, using the previous bound (2.11), we obtain

$$\begin{aligned} \|u_{\varphi_{\varepsilon+h}^*} - u_{\varphi_{\varepsilon}^*} - h v_{\varphi'_{\varepsilon}}, u_{\psi_{\varepsilon+h}^*} - u_{\psi_{\varepsilon}^*} - h v_{\psi'_{\varepsilon}}\|_{(\mathbf{H}^1(\Omega))^2} \\ \leq \frac{|h|}{\varepsilon} C \frac{|h|}{\varepsilon \sqrt{\varepsilon+h}} = C \frac{h^2}{\varepsilon^2 \sqrt{\varepsilon+h}} \xrightarrow{h \rightarrow 0} 0. \end{aligned}$$

To conclude, the continuity of the application  $F'$  follows from an identical proof of the continuity of  $F$ .

3. Let us define  $g(\varepsilon) := \frac{1}{2} |u_{\varphi_{\varepsilon}^*} - u_{\psi_{\varepsilon}^*}|_{\mathbf{H}^1(\Omega)}^2 = \frac{1}{2} \|\nabla(u_{\varphi_{\varepsilon}^*} - u_{\psi_{\varepsilon}^*})\|_{(\mathbf{L}^2(\Omega))^d}^2$ . We have, thanks to the optimality condition for  $(\varphi_{\varepsilon}^*, \psi_{\varepsilon}^*)$  and the system solved by  $(\varphi'_{\varepsilon}, \psi'_{\varepsilon})$ ,

$$\begin{aligned} g'(\varepsilon) &= (\nabla(u_{\varphi_{\varepsilon}^*} - u_{\psi_{\varepsilon}^*}), \nabla(v_{\varphi'_{\varepsilon}} - v_{\psi'_{\varepsilon}}))_{(\mathbf{L}^2(\Omega))^d} \\ &= a((\varphi_{\varepsilon}^*, \psi_{\varepsilon}^*), (\varphi'_{\varepsilon}, \psi'_{\varepsilon})) - \ell(\varphi'_{\varepsilon}, \psi'_{\varepsilon}) \\ &= -\varepsilon \cdot b((\varphi_{\varepsilon}^*, \psi_{\varepsilon}^*), (\varphi'_{\varepsilon}, \psi'_{\varepsilon})) \\ &= \varepsilon \cdot a((\varphi'_{\varepsilon}, \psi'_{\varepsilon}), (\varphi'_{\varepsilon}, \psi'_{\varepsilon})) + \varepsilon^2 \cdot b((\varphi'_{\varepsilon}, \psi'_{\varepsilon}), (\varphi'_{\varepsilon}, \psi'_{\varepsilon})) \\ &= \varepsilon \int_{\Omega} |\nabla v_{\varphi'_{\varepsilon}} - \nabla v_{\psi'_{\varepsilon}}|^2 + \varepsilon^2 \|(v_{\varphi'_{\varepsilon}}, v_{\psi'_{\varepsilon}})\|_{(\mathbf{H}^1(\Omega))^2}^2. \end{aligned}$$

Hence  $g'(\varepsilon) > 0$  if  $\varepsilon > 0$  and we conclude.  $\square$

### 2.3 The case of noisy data: choosing the parameter of regularization with respect to the noise level

As one can expect, in real situations, the data  $(g_N, g_D)$  cannot be measured with complete precision: noise is intrinsically attached with any measurement method. Hence we consider  $(g_N^{\delta}, g_D^{\delta})$  as a measured data which is assumed to satisfy the following condition

$$\|g_D - g_D^{\delta}\|_{\mathbf{H}^{1/2}(\Gamma_{obs})} + \|g_N - g_N^{\delta}\|_{\mathbf{H}^{-1/2}(\Gamma_{obs})} \leq \delta, \quad (2.12)$$

where  $\delta > 0$  is the amplitude of noise on the data. Notice that we do not know if the noisy data  $(g_N^{\delta}, g_D^{\delta})$  is compatible or not.

In the following we explore the convergence of minimizers of the regularized Kohn-Vogelius functional  $\mathcal{K}_{\varepsilon}$  associated to noisy data  $(g_N^{\delta}, g_D^{\delta})$  to the minimum of the Kohn-Vogelius functional without noise, this is, to the solution of the Cauchy problem (1.3). For this we consider the following Kohn-Vogelius functional associated to the noisy data  $(g_N^{\delta}, g_D^{\delta})$ :

$$\mathcal{K}^{\delta}(\varphi, \psi) = \frac{1}{2} \int_{\Omega} |\nabla u_{\varphi}^{g_D^{\delta}} - \nabla u_{\psi}^{g_N^{\delta}}|^2.$$

We also consider its regularization (noticing that the regularization term remains unchanged)

$$\mathcal{K}_{\varepsilon}^{\delta}(\varphi, \psi) = \mathcal{K}^{\delta}(\varphi, \psi) + \frac{\varepsilon}{2} \|(v_{\varphi}, v_{\psi})\|_{(\mathbf{H}^1(\Omega))^2}^2$$

and the associated minimizers  $(\varphi_{\varepsilon, \delta}^*, \psi_{\varepsilon, \delta}^*)$ . We also consider the linear form  $\ell^{\delta}$  associated to the optimality condition for  $(\varphi_{\varepsilon, \delta}^*, \psi_{\varepsilon, \delta}^*)$  and we introduce  $d\ell^{\delta} := \ell^{\delta} - \ell$  which is the linear form associated to  $(dg_N, dg_D) := (g_N^{\delta} - g_N, g_D^{\delta} - g_D)$ . We finally recall that  $(\varphi_{\varepsilon}^*, \psi_{\varepsilon}^*) := \operatorname{argmin}_{(\varphi, \psi)} \mathcal{K}_{\varepsilon}(\varphi, \psi)$ . Moreover, if  $(g_N, g_D)$  is compatible, we note  $(\varphi^*, \psi^*) := \operatorname{argmin}_{(\varphi, \psi)} \mathcal{K}(\varphi, \psi)$ .

### 2.3.1 A convergence result

The key result, in order to obtain the desired convergence from noisy data to the solution of our problem, is the following:

**Proposition 2.9.** *We have*

$$\|(\varphi_{\varepsilon}^*, \psi_{\varepsilon}^*) - (\varphi_{\varepsilon, \delta}^*, \psi_{\varepsilon, \delta}^*)\|_{\mathbb{H}^{-1/2}(\Gamma_i) \times \mathbb{H}^{1/2}(\Gamma_i)} \leq C \frac{\delta}{\sqrt{\varepsilon}}. \quad (2.13)$$

*Proof.* First, notice that

$$\begin{aligned} d\ell^\delta(\varphi, \psi) &= (\ell^\delta - \ell)(\varphi, \psi) = \left( \int_{\Omega} \nabla \left( u^{g_D - g_D^\delta} - u^{g_N - g_N^\delta} \right) \cdot \nabla (v_\varphi - v_\psi) \right) \\ &\leq |u^{g_D - g_D^\delta} - u^{g_N - g_N^\delta}|_{\mathbb{H}^1(\Omega)} |v_\varphi - v_\psi|_{\mathbb{H}^1(\Omega)} \leq C \delta |v_\varphi - v_\psi|_{\mathbb{H}^1(\Omega)}. \end{aligned}$$

Using  $\tilde{\varphi} := \varphi_{\varepsilon, \delta}^* - \varphi_\varepsilon^*$  and  $\tilde{\psi} := \psi_{\varepsilon, \delta}^* - \psi_\varepsilon^*$  in the optimality conditions associated to  $(g_N, g_D)$  and  $(g_N^\delta, g_D^\delta)$  and subtract the obtained equations, we get

$$a((\tilde{\varphi}, \tilde{\psi}), (\tilde{\varphi}, \tilde{\psi})) + \varepsilon \cdot b((\tilde{\varphi}, \tilde{\psi}), (\tilde{\varphi}, \tilde{\psi})) = d\ell(\tilde{\varphi}, \tilde{\psi}).$$

Hence

$$|v_{\tilde{\varphi}} - v_{\tilde{\psi}}|_{\mathbb{H}^1(\Omega)}^2 + \varepsilon \|\tilde{\varphi}, \tilde{\psi}\|_b^2 \leq C \cdot \delta \cdot |v_{\tilde{\varphi}} - v_{\tilde{\psi}}|_{\mathbb{H}^1(\Omega)}$$

and, since  $a^2 + b^2 \geq 2ab$ ,

$$|v_{\tilde{\varphi}} - v_{\tilde{\psi}}|_{\mathbb{H}^1(\Omega)}^2 + \varepsilon \|\tilde{\varphi}, \tilde{\psi}\|_b^2 \geq 2\sqrt{\varepsilon} |v_{\tilde{\varphi}} - v_{\tilde{\psi}}|_{\mathbb{H}^1(\Omega)} \|\tilde{\varphi}, \tilde{\psi}\|_b.$$

Joining the previous results, we obtain

$$\|\tilde{\varphi}, \tilde{\psi}\|_b = \|\varphi_{\varepsilon, \delta}^* - \varphi_\varepsilon^*, \psi_{\varepsilon, \delta}^* - \psi_\varepsilon^*\|_b \leq C \cdot \frac{\delta}{\sqrt{\varepsilon}},$$

which gives the result by the equivalence of norms  $\|\cdot\|_b$  and  $\|\cdot\|_{\mathbb{H}^{-1/2}(\Gamma_i) \times \mathbb{H}^{1/2}(\Gamma_i)}$ .  $\square$

As a corollary, we can deduce in a very general way some conditions on the regularization parameter  $\varepsilon$  in order to have convergence in the noisy case.

**Corollary 2.10.** *Given  $(g_N, g_D)$  compatible data associated to the Kohn-Vogelius functional minimizer  $(\varphi^*, \psi^*)$ . Let us consider  $\varepsilon = \varepsilon(\delta)$  such that*

$$\lim_{\delta \rightarrow 0} \varepsilon(\delta) = 0 \quad \text{and} \quad \lim_{\delta \rightarrow 0} \frac{\delta}{\sqrt{\varepsilon}} = 0. \quad (2.14)$$

*Then we have*

$$\lim_{\delta \rightarrow 0} \|(\varphi_{\varepsilon, \delta}^*, \psi_{\varepsilon, \delta}^*) - (\varphi^*, \psi^*)\|_{\mathbb{H}^{-1/2}(\Gamma_i) \times \mathbb{H}^{1/2}(\Gamma_i)} = 0.$$

*Proof.* This result is direct from the triangle inequality and Theorems 2.6 and 2.9.  $\square$

### 2.3.2 Strategy to choose $\varepsilon$

The last result gives us a guide on how the regularization parameter  $\varepsilon$  should be chosen in order to have convergence to the real solution (when it exists) in the noisy case. However, these conditions are general and do not respond to any precise objective. In this section we explore a well-known criterion for choosing the regularization parameter  $\varepsilon$  based on the definition of a *discrepancy measure*: the so-called *Morozov discrepancy principle* (see [29] for more details in the general regularization of inverse problems context). We follow the same strategy as Ben Belgacem *et al.* in [12] (which is in fact natural with our strategy of considering the Kohn-Vogelius functional).

**Remark 2.11.** *Notice that the choice of our parameter will depend on the noise level  $\delta$  and on the noisy data  $(g_N^\delta, g_D^\delta)$ , this is  $\varepsilon = \varepsilon(\delta, (g_N^\delta, g_D^\delta))$ : it is an a-posteriori choice parameter rule. One may consider an a-priori choice parameter rule which is only based on the noise, that is  $\varepsilon = \varepsilon(\delta)$ . However, in order to obtain optimal order of convergence, one must have some abstract smoothness conditions on the real solution which is, in our opinion, unrealistic in our setting (see [29] for more details on those strategies).*

First, let us assume that our problem has a solution, *i.e.* the Kohn-Vogelius functional  $\mathcal{K}$  associated to the compatible data  $(g_N, g_D)$  has a minimizer  $(\varphi^*, \psi^*)$ . Let us define the *discrepancy measure* as the error in the Kohn-Vogelius functional with noisy data when we evaluate it on the solution of our problem, this is:

$$\begin{aligned} \mathcal{K}^\delta(\varphi^*, \psi^*) &= \frac{1}{2} \int_{\Omega} \left| \nabla \left( u_{\varphi^*}^{g_D^\delta} - u_{\psi^*}^{g_N^\delta} \right) \right|^2 \\ &= \mathcal{K}(\varphi^*, \psi^*) + \frac{1}{2} \int_{\Omega} \left| \nabla \left( u_0^{dg_D} - u_0^{dg_N} \right) \right|^2 \\ &\quad - \int_{\Omega} \nabla \left( u_{\varphi^*}^{g_D} - u_{\psi^*}^{g_N} \right) \cdot \nabla \left( u_0^{dg_D} - u_0^{dg_N} \right), \end{aligned}$$

where the second equality is obtained by rewriting  $u_{\varphi^*}^{g_D^\delta} = u_{\varphi^*}^{g_D^\delta - g_D + g_D} = u_0^{dg_D} + u_{\varphi^*}^{g_D}$  and an analogous expression for  $u_{\psi^*}^{g_N^\delta}$ . Now, as  $(\varphi^*, \psi^*)$  is the minimizer of  $\mathcal{K}$ , we have

$$\mathcal{K}(\varphi^*, \psi^*) = 0 \quad \text{and} \quad \int_{\Omega} \nabla \left( u_{\varphi^*}^{g_D} - u_{\psi^*}^{g_N} \right) \cdot \nabla \left( u_0^{dg_D} - u_0^{dg_N} \right) = 0.$$

From the well-posedness of the problems associated to  $u_0^{dg_D}$  and  $u_0^{dg_N}$  and using (2.12), we obtain

$$\mathcal{K}^\delta(\varphi^*, \psi^*) = \frac{1}{2} \int_{\Omega} \left| \nabla \left( u_0^{dg_D} - u_0^{dg_N} \right) \right|^2 \leq C \delta^2. \quad (2.15)$$

Keeping this in mind, we redefine the noise amount to  $\mathcal{K}^\delta(\varphi^*, \psi^*) = \delta^2$  and we consider the discrepancy principle based on this notion of noise. Notice that this consideration basically says we consider, for the discrepancy principle, that the noise level is taken in a sort of  $H^1 \times H^1$  semi-norm in  $\Omega$  instead of a  $H^{1/2} \times H^{-1/2}$  norm in the inaccessible boundary  $\Gamma_i$ .

By Proposition 2.8, the application  $\varepsilon \mapsto \mathcal{K}^\delta(\varphi_{\varepsilon, \delta}^*, \psi_{\varepsilon, \delta}^*)$  is strictly increasing and therefore injective. Moreover, it is easy to see that if  $\varepsilon \in [0, \infty)$  then  $\mathcal{K}^\delta(\varphi_{\varepsilon, \delta}^*, \psi_{\varepsilon, \delta}^*) \in [0, \mathcal{K}^\delta(0, 0))$ . Let us assume that there exists  $\tau > 1$  such that  $\tau \delta^2 \in [0, \mathcal{K}^\delta(0, 0))$ . This is natural as we expect that the data we have is not of the same order as the noise: otherwise  $(\varphi^*, \psi^*) = (0, 0)$



would be an *admissible* approximation of the exact solution. So, the discrepancy principle consists, in our case, on choosing  $\varepsilon$  such that

$$\varepsilon = \sup \left\{ \varepsilon : \mathcal{K}^\delta(\varphi_{\varepsilon,\delta}^*, \psi_{\varepsilon,\delta}^*) \leq \tau \delta^2 \right\}. \quad (2.16)$$

The idea of choosing the sup is based on the fact that a small regularization parameter involves less stability, so the *natural* strategy is to choose the biggest regularization parameter such that the discrepancy is in the order of the noise. The injectivity and increasing monotonicity of the application  $\mathcal{K}^\delta$  implies that  $\varepsilon$  is simply the parameter such that

$$\mathcal{K}^\delta(\varphi_{\varepsilon,\delta}^*, \psi_{\varepsilon,\delta}^*) = \tau \delta^2. \quad (2.17)$$

**Remark 2.12.** *It is important to notice that the “redefinition” of the noise estimate does not involve, for real computations, the knowledge of the real solution  $(\varphi^*, \psi^*)$ . In fact, we only use the real solution when we evaluate it into the Kohn-Vogelius functional with noisy data  $(g_N^\delta, g_D^\delta)$  obtaining the estimate (2.15). We can observe that this quantity only depends on a constant  $C$  and the error estimate  $\delta$ . Hence, by assuming that  $C \leq 1$  (which is itself a strong assumption, as  $C$  depends on Poincaré inequality constant and trace theorem constant<sup>2</sup>), we can consider  $\mathcal{K}^\delta(\varphi^*, \psi^*) = \delta^2$  as the error measure between the real and measured data which leads to the discrepancy principle formulation given by (2.16).*

Now we prove that this *a posteriori* choice parameter rule satisfies the conditions of Corollary 2.10.

**Proposition 2.13.** *The regularization parameter choice given by the Morozov discrepancy principle (2.17) satisfies*

$$\lim_{\delta \rightarrow 0} \varepsilon(\delta) = 0 \quad \text{and} \quad \lim_{\delta \rightarrow 0} \frac{\delta}{\sqrt{\varepsilon}} = 0.$$

*This implies, in particular, that we have the following convergence*

$$\lim_{\delta \rightarrow 0} \|(\varphi_{\varepsilon,\delta}^*, \psi_{\varepsilon,\delta}^*) - (\varphi^*, \psi^*)\|_{\mathbf{H}^{-1/2}(\Gamma_i) \times \mathbf{H}^{1/2}(\Gamma_i)} = 0.$$

*Proof.* The first condition is obvious from the definition of  $\varepsilon$ . Given  $\varepsilon$  computed by the discrepancy principle (2.17). By definition

$$\begin{aligned} \mathcal{K}_\varepsilon^\delta(\varphi_{\varepsilon,\delta}^*, \psi_{\varepsilon,\delta}^*) &\leq \mathcal{K}_\varepsilon^\delta(\varphi^*, \psi^*) \\ \iff \frac{\varepsilon}{2} \|(\varphi_{\varepsilon,\delta}^*, \psi_{\varepsilon,\delta}^*)\|_b^2 + \mathcal{K}^\delta(\varphi_{\varepsilon,\delta}^*, \psi_{\varepsilon,\delta}^*) &\leq \frac{\varepsilon}{2} \|(\varphi^*, \psi^*)\|_b^2 + \mathcal{K}^\delta(\varphi^*, \psi^*) \end{aligned}$$

and then, using (2.15),

$$\frac{\varepsilon}{2} \|(\varphi_{\varepsilon,\delta}^*, \psi_{\varepsilon,\delta}^*)\|_b^2 + \tau \delta^2 \leq \frac{\varepsilon}{2} \|(\varphi^*, \psi^*)\|_b^2 + \delta^2.$$

Rearranging terms, we obtain for all  $\delta > 0$

$$0 < 2(\tau - 1) \frac{\delta^2}{\varepsilon} \leq \|(\varphi^*, \psi^*)\|_b^2 - \|(\varphi_{\varepsilon,\delta}^*, \psi_{\varepsilon,\delta}^*)\|_b^2.$$

Hence it suffices to prove

$$\lim_{\delta \rightarrow 0} \|(\varphi_{\varepsilon,\delta}^*, \psi_{\varepsilon,\delta}^*)\|_b = \|(\varphi^*, \psi^*)\|_b.$$

---

<sup>2</sup>The estimation of the constant  $C$  should be analyzed in detail but is beyond the scope of this work

To this, first notice that for all  $\delta > 0$

$$\|(\varphi_{\varepsilon,\delta}^*, \psi_{\varepsilon,\delta}^*)\|_b \leq \|(\varphi^*, \psi^*)\|_b. \quad (2.18)$$

In particular

$$\limsup_{\delta \rightarrow 0} \|(\varphi_{\varepsilon,\delta}^*, \psi_{\varepsilon,\delta}^*)\|_b \leq \|(\varphi^*, \psi^*)\|_b. \quad (2.19)$$

Now, take a sequence  $(\delta_n)_n \xrightarrow{n \rightarrow \infty} 0$ . By (2.18),  $(\varphi_{\varepsilon,\delta_n}^*, \psi_{\varepsilon,\delta_n}^*)_n$  is bounded in  $(\mathbf{H}^{-1/2}(\Gamma_i) \times \mathbf{H}^{1/2}(\Gamma_i), \|\cdot\|_b)$ . Hence, there exists  $(\tilde{\varphi}, \tilde{\psi}) \in \mathbf{H}^{-1/2}(\Gamma_i) \times \mathbf{H}^{1/2}(\Gamma_i)$  such that, up to a subsequence,  $(\varphi_{\varepsilon,\delta_n}^*, \psi_{\varepsilon,\delta_n}^*)_n \rightharpoonup (\tilde{\varphi}, \tilde{\psi})$  weakly in  $\mathbf{H}^{-1/2}(\Gamma_i) \times \mathbf{H}^{1/2}(\Gamma_i)$ .

Now, let us prove that  $(\tilde{\varphi}, \tilde{\psi}) = (\varphi^*, \psi^*)$ . To this, it suffices to prove that  $(\tilde{\varphi}, \tilde{\psi})$  satisfies (2.4) (see [31, Proposition 1.7]). Let us consider the optimality condition (2.8) which is satisfied by the sequence  $(\varphi_{\varepsilon,\delta_n}^*, \psi_{\varepsilon,\delta_n}^*)_n$ :

$$a((\varphi_{\varepsilon,\delta_n}^*, \psi_{\varepsilon,\delta_n}^*), (\varphi, \psi)) + \varepsilon \cdot b((\varphi_{\varepsilon,\delta_n}^*, \psi_{\varepsilon,\delta_n}^*), (\varphi, \psi)) = \ell^{(g_N^{\delta_n}, g_D^{\delta_n})}(\varphi, \psi).$$

The linear form  $a((\cdot, \cdot), (\varphi, \psi))$  is continuous, the second term converges to zero and the right-hand side term converges to  $\ell^{(g_N, g_D)}(\varphi, \psi)$  thanks to:

$$|\ell^{(g_N^{\delta_n}, g_D^{\delta_n})}(\varphi, \psi) - \ell^{(g_N, g_D)}(\varphi, \psi)| = \int_{\Omega} \nabla(v_{\varphi} - v_{\psi}) \cdot \nabla(u_0^{g_N^{\delta_n} - g_N} - u_0^{g_D^{\delta_n} - g_D}) \leq C\|(\varphi, \psi)\| \cdot \delta.$$

Hence, passing to the limit,

$$a((\tilde{\varphi}, \tilde{\psi}), (\varphi, \psi)) = \ell^{(g_N, g_D)}(\varphi, \psi), \quad \forall (\varphi, \psi) \in \mathbf{H}^{-1/2}(\Gamma_i) \times \mathbf{H}^{1/2}(\Gamma_i)$$

and we conclude  $(\tilde{\varphi}, \tilde{\psi}) = (\varphi^*, \psi^*)$ .

Finally, the strong continuity of the norm implies the weak lower-semicontinuity and then

$$\|(\varphi^*, \psi^*)\|_b \leq \liminf_n \|(\varphi_{\varepsilon,\delta}^*, \psi_{\varepsilon,\delta}^*)\|_b.$$

Since the sequence used is arbitrary, we conclude combining this inequality with (2.19).  $\square$

## 2.4 Numerical simulations concerning the data completion problem

### 2.4.1 Computation of the derivatives of $\mathcal{K}_{\varepsilon}$

In order to perform the numerical minimization of the regularized functional  $\mathcal{K}_{\varepsilon}$  via a gradient algorithm we have to compute its derivatives with respect to  $\varphi$  and  $\psi$ .

**Proposition 2.14.** *For all  $(\varphi, \psi), (\tilde{\varphi}, \tilde{\psi}) \in \mathbf{H}^{-1/2}(\Gamma_i) \times \mathbf{H}^{1/2}(\Gamma_i)$ , the partial derivative of the functional  $\mathcal{K}_{\varepsilon}$  are given by*

$$\frac{\partial \mathcal{K}_{\varepsilon}}{\partial \varphi}(\varphi, \psi) [\tilde{\varphi}] = \int_{\Gamma_i} \tilde{\varphi} \cdot (u_{\varphi} + \varepsilon v_{\varphi} + w_D - \psi) \quad (2.20)$$

and

$$\frac{\partial \mathcal{K}_{\varepsilon}}{\partial \psi}(\varphi, \psi) [\tilde{\psi}] = \langle (\partial_{\nu} u_{\psi} + \varepsilon \partial_{\nu} v_{\psi} + \partial_{\nu} w_N - \varphi), \tilde{\psi} \rangle_{-1/2, 1/2, \Gamma_i} \quad (2.21)$$

where  $w_N, w_D \in \mathbf{H}^1(\Omega)$  are the respective solutions of the following adjoint problems:

$$\left\{ \begin{array}{ll} -\Delta w_N = -\varepsilon v_{\psi} & \text{in } \Omega \\ \partial_{\nu} w_N = \partial_{\nu} u_{\varphi} - g_N & \text{on } \Gamma_{obs} \\ w_N = 0 & \text{on } \Gamma_i \end{array} \right. \quad \text{and} \quad \left\{ \begin{array}{ll} -\Delta w_D = \varepsilon v_{\varphi} & \text{in } \Omega \\ w_D = u_{\psi} - g_D & \text{on } \Gamma_{obs} \\ \partial_{\nu} w_D = 0 & \text{on } \Gamma_i. \end{array} \right. \quad (2.22)$$

In particular, the directions  $(\tilde{\varphi}, \tilde{\psi}) \in \mathbf{H}^{-1/2}(\Gamma_i) \times \mathbf{H}^{1/2}(\Gamma_i)$  given by:

$$\tilde{\varphi} = \psi - u_\varphi|_{\Gamma_i} - \varepsilon v_\varphi|_{\Gamma_i} - w_D|_{\Gamma_i}, \quad (2.23)$$

and

$$\tilde{\psi} = -v_W|_{\Gamma_i}, \quad (2.24)$$

with  $W := \varphi - \partial_\nu u_\psi|_{\Gamma_i} - \varepsilon \partial_\nu v_\psi|_{\Gamma_i} - \partial_\nu w_N|_{\Gamma_i} \in \mathbf{H}^{-1/2}(\Gamma_i)$ , are descent directions.

We recall that  $v_\varphi, v_\psi \in \mathbf{H}^1(\Omega)$  are the solutions of Problems (2.3).

*Proof.* Let  $(\varphi, \psi), (\tilde{\varphi}, \tilde{\psi}) \in \mathbf{H}^{-1/2}(\Gamma_i) \times \mathbf{H}^{1/2}(\Gamma_i)$ . Easy computations gives

$$\frac{\partial \mathcal{K}_\varepsilon}{\partial \varphi}(\varphi, \psi) [\tilde{\varphi}] = \int_\Omega \nabla v_{\tilde{\varphi}} \cdot (\nabla u_\varphi + \varepsilon \nabla v_\varphi - \nabla u_\psi) + \varepsilon \int_\Omega v_{\tilde{\varphi}} v_\varphi \quad (2.25)$$

and

$$\frac{\partial \mathcal{K}_\varepsilon}{\partial \psi}(\varphi, \psi) [\tilde{\psi}] = \int_\Omega \nabla v_{\tilde{\psi}} \cdot (\nabla u_\psi + \varepsilon \nabla v_\psi - \nabla u_\varphi) + \varepsilon \int_\Omega v_{\tilde{\psi}} v_\psi. \quad (2.26)$$

Then, using Green formula in the adjoint problem solved by  $w_N$  (see (2.22)) and in problem solved by  $v_{\tilde{\psi}}$  (see (2.3)) and in the adjoint problem solved by  $w_D$  (see (2.22)) and in problem solved by  $v_{\tilde{\varphi}}$  (see (2.3)), we get

$$\int_{\Gamma_i} \tilde{\psi} \partial_\nu w_N = \varepsilon \int_\Omega v_\psi v_{\tilde{\psi}} + \int_{\Gamma_{obs}} v_{\tilde{\psi}} (g_N - \partial_\nu u_\varphi)$$

and

$$\int_{\Gamma_i} \tilde{\varphi} w_D = \varepsilon \int_\Omega v_\varphi v_{\tilde{\varphi}} + \int_{\Gamma_{obs}} \partial_\nu v_{\tilde{\varphi}} (g_D - u_\psi).$$

Thus, from the expression (2.25), we get

$$\frac{\partial \mathcal{K}_\varepsilon}{\partial \varphi}(\varphi, \psi) [\tilde{\varphi}] = \int_{\partial \Omega} \partial_\nu v_{\tilde{\varphi}} (u_\varphi + \varepsilon v_\varphi - u_\psi) + \varepsilon \int_\Omega v_{\tilde{\varphi}} v_\varphi = \int_{\Gamma_i} \tilde{\varphi} (u_\varphi + \varepsilon v_\varphi - u_\psi + w_D).$$

With an analogous procedure for (2.26) we obtain (2.21).

Is important to remark that the formula for  $\tilde{\varphi}$  should be understood as the representative of the natural linear functional associated to the given expression (which is in  $\mathbf{H}^{1/2}(\Gamma_i)$ ) in order to be understood in the proper space. For the descent direction  $\tilde{\psi}$ , we should notice that

$$\frac{\partial \mathcal{K}_\varepsilon}{\partial \psi} [\tilde{\psi}] = \langle W, \tilde{\psi} \rangle.$$

However, from the variational formulation of  $v_W$ , we have, for all  $u \in \mathbf{H}^1(\Omega)$  such that  $u|_{\Gamma_{obs}} = 0$ ,

$$\int_\Omega \nabla v_W \cdot \nabla u = \langle W, u \rangle.$$

Hence, taking  $u = -v_W$ , we obtain

$$- \int_\Omega |\nabla v_W|^2 = \langle W, -v_W \rangle < 0,$$

and we conclude.  $\square$

### 2.4.2 Framework of the numerical simulations

To make the numerical simulations presented here, we use a  $P1$  finite elements discretization to solve the Laplace's equations (2.2) and (2.3), and Poisson's equations (2.22) related to the adjoint states.

The framework is the following: the exterior boundary is assumed to be the border of the square  $\Omega = [-0.5, 0.5] \times [-0.5, 0.5]$ . Except when mentioned, we consider here  $\Gamma_{obs} = ([-0.5, 0.5] \times \{-0.5\}) \cup (\{-0.5\} \times [-0.5, 0.5]) \cup (\{0.5\} \times [-0.5, 0.5])$  and  $\Gamma_i = [-0.5, 0.5] \times \{0.5\}$ . The Cauchy data  $(g_N, g_D)$  is the trace and normal derivative of the harmonic function  $u(x, y) = y^3 - 3x^2y$ . The inclusion of noise will depend on the test itself and will be described below. Finally, we remark that Problems (2.2), (2.3), (2.22) are well posed in this case, following the results of Savare [45] and noticing that in this case the angle in which the boundaries meet is  $\pi/2 \in [0, \pi)$ .

In order to update the construction of  $(\varphi, \psi)$  to approach  $(\varphi_\varepsilon^*, \psi_\varepsilon^*)$ , we follow a gradient algorithm, for which the descent directions are given in detail in Proposition 2.14.

#### Algorithm

1. Let  $k = 0$ . Fix  $k_{max}$  (max. number of iterations) and  $tol$  (tolerance), choose  $(\varphi_0, \psi_0)$  as the initial guess of the missing data.
2. Solve Problems (2.2) with  $(\varphi_k, \psi_k)$ , extract the solutions  $u_{\varphi_k}, u_{\psi_k}$  and compute  $\mathcal{K}(\varphi_k, \psi_k)$ .
  - If  $\mathcal{K}(\varphi_k, \psi_k) < tol$ : STOP.
  - Else: continue to next step.
3. Solve Problems (2.3), (2.22) with  $(\varphi_k, \psi_k)$ , extract the solutions  $v_{\varphi_k}, v_{\psi_k}, w_N(\varphi_k, \psi_k)$  and  $w_D(\varphi_k, \psi_k)$ .
4. Compute the descent directions  $\tilde{\varphi}, \tilde{\psi}$  using formulas (2.23), (2.24) with  $(\varphi_k, \psi_k)$  and the solutions given in steps 2 and 3.
5. Update  $\varphi_k \leftarrow (\varphi_k - \alpha_1 \tilde{\varphi}), \psi_k \leftarrow (\psi_k - \alpha_2 \tilde{\psi})$ .
6. While  $k \leq k_{max}$  and  $\mathcal{K}_\varepsilon(\varphi_k, \psi_k) - \mathcal{K}_\varepsilon(\varphi_{k-1}, \psi_{k-1}) < tol$ , get back to the step 2,  $k \leftarrow k + 1$ .

The step lengths  $\alpha_1, \alpha_2$  are set as fixed parameters in our simulations with  $\alpha_1 = \alpha_2 = 0.01$ , the maximum number of iterations  $k_{max}$  is set to 100 and the tolerance  $tol$  for the functional is set to 0.1. In the case when noise is considered into the measurements, it is considered in the following way: given a measure  $g$  in a region  $O \subset \partial\Omega$ , we introduce the noisy version of  $g$ , denoted  $g^\sigma$ , as:

$$g^\sigma := g + \sigma \frac{\|g\|_{L^2(O)}}{\|u\|_{L^2(O)}} u,$$

where  $u$  is a random variable given by an uniform distribution in  $[0, 1)$  and  $\sigma > 0$  is a scaling parameter. Notice that this definition implies that the data  $g$  is contaminated by some relative error of amplitude  $\sigma$  in  $L^2(O)$ . So, the noisy data into  $\Gamma_{obs}$  will be  $(g_N^\sigma, g_D^\sigma)$ . In this work we consider  $\sigma = 0.05$ , which corresponds to a noise of 5% with respect to the original measurements.

To conclude, we precise that we have used the finite elements library FREEFEM++ (see [37]) to make the simulations. We present several simulations, with or without noise, in the following subsections and comment these results in Subsection 2.4.5.

### 2.4.3 Numerical simulations without noise

Under the considerations given in the previous section we present the results of the above algorithm in the case where the data  $(g_N, g_D)$  is free from noise. Here we consider  $(\varphi_0, \psi_0) = (\partial_\nu u_{ex} - 0.1, -x^2)$  and  $\varepsilon$  is tested for several values. We summarize the obtained results in Figure 2 and Table 1. The results show that the algorithm is capable to reduce the error

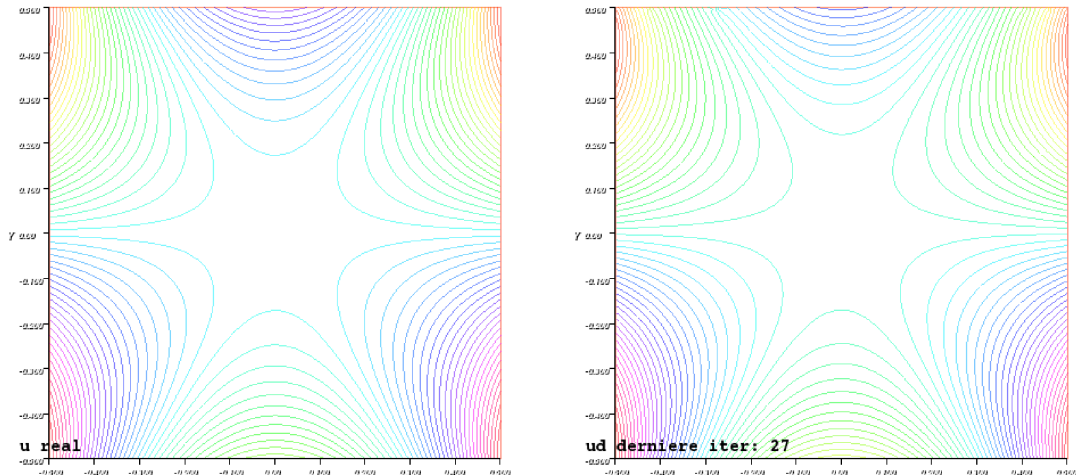


Figure 2: Non noisy case (Left: real solution. Right: obtained solution after 27 iterations.)

Table 1: Non noisy case

|                       |       | initial error ( $k = 0$ ) | $\varepsilon = 0.1$ | $\varepsilon = 0.01$ | $\varepsilon = 0.001$ |
|-----------------------|-------|---------------------------|---------------------|----------------------|-----------------------|
| $L^2(\Omega)$ error   | $u_D$ | 0.0450                    | 0.0343              | 0.0272               | 0.0255                |
|                       | $u_N$ | 0.1244                    | 0.0857              | 0.0860               | 0.0860                |
| $L^2(\Gamma_i)$ error | $u_D$ | 0.0401                    | 0.0411              | 0.0390               | 0.0381                |
|                       | $u_N$ | 0.1679                    | 0.0975              | 0.0985               | 0.0984                |

from the first guess in order to approximate the real solution. We can also observe that the regularization parameter  $\varepsilon$  should be adjusted in order to obtain better results.

### 2.4.4 Numerical simulations with noise

Now we want to observe if the addition of noise generates dramatic changes in the solution, as it happens in the non-regularized case due to the ill-posedness of the problem. Under the same considerations as in the non-noisy case, we obtain the results given in Figure 3 and Table 2. Here again, the reconstruction of the data (and of the solution) is effective.

Table 2: Noisy case (5%).

| Case $\overline{\Gamma_{obs}} \cap \overline{\Gamma_i} \neq \emptyset$ |       | initial error ( $k = 0$ ) | $\varepsilon = 0.1$ | $\varepsilon = 0.01$ | $\varepsilon = 0.001$ |
|--|-------|---------------------------|---------------------|----------------------|-----------------------|
| $L^2(\Omega)$ error  | $u_D$ | 0.0798                    | 0.0221              | 0.0315               | 0.0096                |
|  | $u_N$ | 0.1534                    | 0.0873              | 0.0856               | 0.0865                |
| $L^2(\Gamma_i)$ error  | $u_D$ | 0.0541                    | 0.0359              | 0.0452               | 0.0340                |
|  | $u_N$ | 0.1679                    | 0.1030              | 0.0971               | 0.1003                |

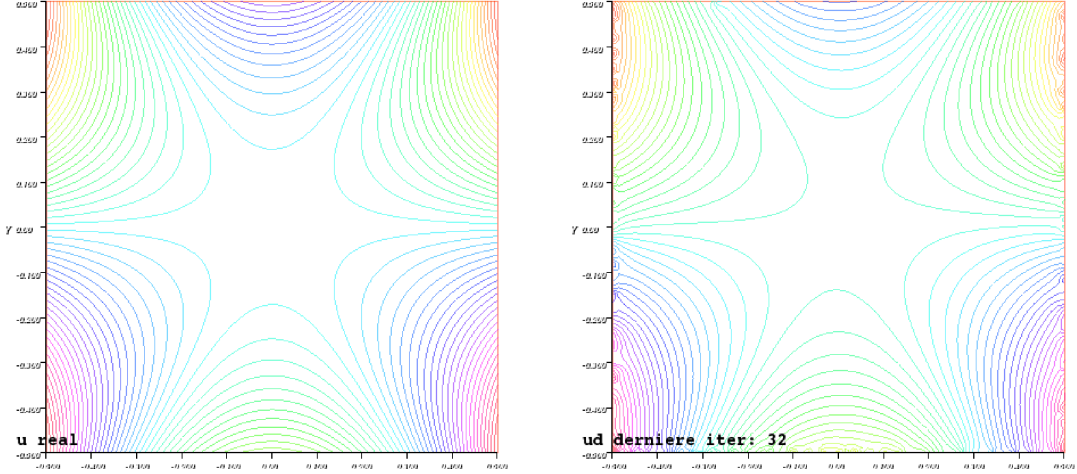


Figure 3: Noisy case (5%) (Left: real solution. Right: obtained solution after 32 iterations.)

### 2.4.5 Comments on the simulations

The exposed examples show that our algorithm is effective to improve the guess  $(\varphi_0, \psi_0)$  in order to approximate the data to the real one. We can also observe that the regularization parameter  $\varepsilon$  reveals better results for the values  $10^{-2}$  and  $10^{-3}$ . This is in concordance with the results obtained in [7] which also reveals that the regularization is effective in order to avoid big errors in the obtained solutions when noise is introduced to the accessible data.

## 3 The inverse obstacle problem with partial Cauchy data

We now focus on the numerical reconstruction of an unknown object  $\omega^*$  (*i.e.* the obstacle), included into the domain of study  $\Omega$ , which is characterized by an homogeneous Dirichlet boundary condition, only from the knowledge of the Cauchy data  $(g_N, g_D)$  measured into the observable part  $\Gamma_{obs}$  of  $\partial\Omega$ . We recall that in order to study this initial inverse problem (1.1), we focus on the optimization problem (1.4). However, taking into account our previous theoretical study of the data completion problem, we have to regularize the Kohn-Vogelius functional  $\mathcal{K}$ . Hence, in the following, we consider, instead of (1.4), the following optimization problem

$$(\omega^*, \varphi^*, \psi^*) \in \underset{(\omega, \varphi, \psi) \in \mathcal{D} \times H^{-1/2}(\Gamma_i) \times H^{1/2}(\Gamma_i)}{\operatorname{argmin}} \mathcal{K}_\varepsilon(\omega, \varphi, \psi)$$

where the set of admissible geometries  $\mathcal{D}$  is given by (1.2) and where  $\mathcal{K}_\varepsilon$  is the regularized nonnegative Kohn-Vogelius cost functional defined by

$$\begin{aligned} \mathcal{K}_\varepsilon(\omega, \varphi, \psi) &:= \mathcal{K}(\omega, \varphi, \psi) + \frac{\varepsilon}{2} \|(v_\varphi, v_\psi)\|_{(H^1(\Omega \setminus \bar{\omega}))^2}^2 \\ &= \frac{1}{2} \int_{\Omega \setminus \bar{\omega}} |\nabla u_\varphi - \nabla u_\psi|^2 + \frac{\varepsilon}{2} \|(v_\varphi, v_\psi)\|_{(H^1(\Omega \setminus \bar{\omega}))^2}^2, \end{aligned}$$

where  $u_\varphi, u_\psi \in H^1(\Omega \setminus \bar{\omega})$  and  $v_\varphi, v_\psi \in H^1(\Omega \setminus \bar{\omega})$  are the respective solutions of Problems (1.6) and (1.7).

To minimize the functional  $\mathcal{K}_\varepsilon$ , we first compute the gradient in order to make a descent method to reconstruct numerically the solution. The partial derivatives with respect to  $\varphi$  and  $\psi$  are given by Proposition 2.14 and we compute the shape gradient in the following subsection.

### 3.1 Shape derivative of the Kohn-Vogelius functional

We also define  $\Omega_{d_0}$  an open set with a  $C^\infty$  boundary such that

$$\{x \in \Omega; d(x, \partial\Omega) > d_0/2\} \subset \Omega_{d_0} \subset \{x \in \Omega; d(x, \partial\Omega) > d_0/3\}.$$

In order to define the shape derivatives, we will use the *velocity method* introduced by Murat and Simon in [42]. To this end, we need to introduce the following space of admissible deformations

$$\mathbf{U} := \left\{ \mathbf{V} \in \mathbf{W}^{2,\infty}(\mathbb{R}^d); \text{Supp } \mathbf{V} \subset \overline{\Omega_{d_0}} \right\}.$$

In particular we are interested in the shape gradient of  $\mathcal{K}_\varepsilon$  defined by

$$\text{DK}_\varepsilon(\omega) \cdot \mathbf{V} := \lim_{t \rightarrow 0} \frac{\mathcal{K}_\varepsilon((\mathbf{I} + t\mathbf{V})(\omega)) - \mathcal{K}_\varepsilon(\omega)}{t}.$$

For details concerning the differentiation with respect to the domain, we refer to the papers of Simon [46, 47] and the books of Henrot and Pierre [38] and of Sokółowski and Zolésio [48]. We precise that we omit to precise the dependance with respect to  $\varphi$  and  $\psi$  in this section, that is we write  $\mathcal{K}_\varepsilon(\omega)$  instead of  $\mathcal{K}_\varepsilon(\omega, \varphi, \psi)$ .

We consider a domain  $\omega \in \mathcal{D}$ . Then we have the following proposition.

**Proposition 3.1** (First order shape derivative of the functional). *For  $\mathbf{V} \in \mathbf{U}$ , the regularized Kohn-Vogelius cost functional  $\mathcal{K}_\varepsilon$  is differentiable at  $\omega$  in the direction  $\mathbf{V}$  with*

$$\begin{aligned} \text{DK}_\varepsilon(\omega) \cdot \mathbf{V} = & - \int_{\partial\omega} (\partial_\nu \rho_N^u \cdot \partial_\nu u_\varphi + \partial_\nu \rho_N^v \cdot \partial_\nu v_\varphi)(\mathbf{V} \cdot \nu) + \frac{1}{2} \int_{\partial\omega} |\nabla w|^2 (\mathbf{V} \cdot \nu) \\ & - \int_{\partial\omega} (\partial_\nu \rho_D^u \cdot \partial_\nu u_\psi + \partial_\nu \rho_D^v \cdot \partial_\nu v_\psi)(\mathbf{V} \cdot \nu) \\ & + \frac{\varepsilon}{2} \int_{\partial\omega} (|\nabla v_\varphi|^2 + |\nabla v_\psi|^2 + |v_\varphi|^2 + |v_\psi|^2)(\mathbf{V} \cdot \nu), \end{aligned} \quad (3.1)$$

where  $w := u_\varphi - u_\psi$  and where  $\rho_D^u, \rho_N^u, \rho_D^v, \rho_N^v \in \text{H}^1(\Omega \setminus \bar{\omega})$  are the respective solutions of the following adjoint problems

$$\left\{ \begin{array}{ll} -\Delta \rho_N^u = 0 & \text{in } \Omega \setminus \bar{\omega} \\ \rho_N^u = g_D - u_\psi & \text{on } \Gamma_{obs} \\ \partial_\nu \rho_N^u = 0 & \text{on } \Gamma_i \\ \rho_N^u = 0 & \text{on } \partial\omega, \end{array} \right. \quad \left\{ \begin{array}{ll} -\Delta \rho_N^v = -\varepsilon v_\varphi & \text{in } \Omega \setminus \bar{\omega} \\ \rho_N^v = 0 & \text{on } \Gamma_{obs} \\ \partial_\nu \rho_N^v = 0 & \text{on } \Gamma_i \\ \rho_N^v = 0 & \text{on } \partial\omega \end{array} \right. \quad (3.2)$$

and

$$\left\{ \begin{array}{ll} -\Delta \rho_D^u = 0 & \text{in } \Omega \setminus \bar{\omega} \\ \partial_\nu \rho_D^u = 0 & \text{on } \Gamma_{obs} \\ \rho_D^u = \psi - u_\varphi & \text{on } \Gamma_i \\ \rho_D^u = 0 & \text{on } \partial\omega, \end{array} \right. \quad \left\{ \begin{array}{ll} -\Delta \rho_D^v = -\varepsilon v_\psi & \text{in } \Omega \setminus \bar{\omega} \\ \partial_\nu \rho_D^v = 0 & \text{on } \Gamma_{obs} \\ \rho_D^v = \varepsilon \psi & \text{on } \Gamma_i \\ \rho_D^v = 0 & \text{on } \partial\omega. \end{array} \right. \quad (3.3)$$

*Proof.* First, notice that the existence of the shape derivatives  $u'_\varphi, v'_\varphi, u'_\psi, v'_\psi \in \text{H}^1(\Omega \setminus \bar{\omega})$  is standard and is based on Implicit function theorem. We refer to [38, Chapter 5] for details (see also [8] for example). Moreover, these shape derivatives are respectively characterized as the solution of the following problems (see again [38, Chapter 5]):

$$\left\{ \begin{array}{ll} -\Delta u'_\varphi = 0 & \text{in } \Omega \setminus \bar{\omega} \\ u'_\varphi = 0 & \text{on } \Gamma_{obs} \\ \partial_\nu u'_\varphi = 0 & \text{on } \Gamma_i \\ u'_\varphi = -\partial_\nu u_\varphi(\mathbf{V} \cdot \nu) & \text{on } \partial\omega, \end{array} \right. \quad \left\{ \begin{array}{ll} -\Delta v'_\varphi = 0 & \text{in } \Omega \setminus \bar{\omega} \\ v'_\varphi = 0 & \text{on } \Gamma_{obs} \\ \partial_\nu v'_\varphi = 0 & \text{on } \Gamma_i \\ v'_\varphi = -\partial_\nu v_\varphi(\mathbf{V} \cdot \nu) & \text{on } \partial\omega \end{array} \right. \quad (3.4)$$

and

$$\left\{ \begin{array}{ll} -\Delta u'_\psi = 0 & \text{in } \Omega \setminus \bar{\omega} \\ \partial_\nu u'_\psi = 0 & \text{on } \Gamma_{obs} \\ u'_\psi = 0 & \text{on } \Gamma_i \\ u'_\psi = -\partial_\nu u_\psi(\mathbf{V} \cdot \nu) & \text{on } \partial\omega, \end{array} \right. \quad \left\{ \begin{array}{ll} -\Delta v'_\psi = 0 & \text{in } \Omega \setminus \bar{\omega} \\ \partial_\nu v'_\psi = 0 & \text{on } \Gamma_{obs} \\ v'_\psi = 0 & \text{on } \Gamma_i \\ v'_\psi = -\partial_\nu v_\psi(\mathbf{V} \cdot \nu) & \text{on } \partial\omega. \end{array} \right. \quad (3.5)$$

Introducing  $w := u_\varphi - u_\psi$  and  $w' := u'_\varphi - u'_\psi$ , we use Hadamard formula (see [38, Theorem 5.2.2]) to get

$$\begin{aligned} DK_\varepsilon(\Omega \setminus \bar{\omega}) \cdot \mathbf{V} &= \int_{\Omega \setminus \bar{\omega}} \nabla w' \cdot \nabla w + \frac{1}{2} \int_{\partial\omega} |\nabla w|^2 (\mathbf{V} \cdot \nu) \\ &\quad + \varepsilon \int_{\Omega \setminus \bar{\omega}} (\nabla v'_\varphi \cdot \nabla v_\varphi + \nabla v'_\psi \cdot \nabla v_\psi + v'_\varphi v_\varphi + v'_\psi v_\psi) \\ &\quad + \frac{\varepsilon}{2} \int_{\partial\omega} (|\nabla v_\varphi|^2 + |\nabla v_\psi|^2 + |v_\varphi|^2 + |v_\psi|^2) (\mathbf{V} \cdot \nu). \end{aligned}$$

Using Green formula into the variational formulation of (3.2) and (3.4) and of (3.3) and (3.7) respectively, we obtain:

$$\begin{aligned} \int_{\Omega \setminus \bar{\omega}} \nabla w \cdot \nabla u'_\varphi + \varepsilon \int_{\Omega \setminus \bar{\omega}} (\nabla v'_\varphi \cdot \nabla v_\varphi + v'_\varphi \cdot v_\varphi) &= - \int_{\partial\omega} \partial_\nu \rho_N^u \cdot \partial_\nu u_\varphi (\mathbf{V} \cdot \nu) \\ &\quad - \int_{\partial\omega} \partial_\nu \rho_N^v \cdot \partial_\nu v_\varphi (\mathbf{V} \cdot \nu) \end{aligned}$$

and

$$\begin{aligned} - \int_{\Omega \setminus \bar{\omega}} \nabla w \cdot \nabla u'_\psi + \varepsilon \int_{\Omega \setminus \bar{\omega}} (\nabla v'_\psi \cdot \nabla v_\psi + v'_\psi \cdot v_\psi) &= - \int_{\partial\omega} \partial_\nu \rho_D^u \cdot \partial_\nu u_\psi (\mathbf{V} \cdot \nu) \\ &\quad - \int_{\partial\omega} \partial_\nu \rho_D^v \cdot \partial_\nu v_\psi (\mathbf{V} \cdot \nu), \end{aligned}$$

which concludes the proof.  $\square$

### 3.2 Framework for the numerical simulations

Theorem 2 in [3] explains the difficulties encountered to solve numerically the reconstruction of  $\omega$ . Indeed, the shape gradient has not an uniform sensitivity with respect to the deformation direction. Hence, since the inverse obstacle problem is severely ill-posed, we need some regularization methods to solve it numerically, for example by adding to the functional a penalization in terms of the perimeter (see [17] or [25]). Here, we choose to make a regularization by parametrization using a parametric model of shape variations.

As before, all the involved systems are discretized using  $P1$  finite elements. The framework is the same as in Section 2.4.2 for the domain  $\Omega$ , the boundaries  $\Gamma_{obs}$  and  $\Gamma_i$  and the initial guess  $(\varphi_0, \psi_0)$ . The real object  $\omega^*$  is detailed on each simulation, as well as their initial guess  $\omega_0$ . In order to have a suitable pair of Cauchy data and real domain  $\omega^*$ , we use synthetic data: we fix a shape  $\omega^*$ , we solve the Laplace's equation in  $\Omega \setminus \bar{\omega}^*$  with an explicit data  $g_D$  (or  $g_N$ ) over  $\partial\Omega$  and homogeneous Dirichlet boundary condition over  $\partial\omega$  by means of another finite element method (here a  $P2$  finite element discretization) from where we extract the corresponding data  $g_N$  (or  $g_D$ ) by computing the value  $\partial_\nu u$  (or  $u$ ) on  $\Gamma_{obs}$ .



For the obstacle numerical reconstruction, we follow the same strategy than in [3] or in [22] that we recall for readers convenience. We restrict ourselves to star-shaped domains and use polar coordinates for parametrization: the boundary  $\partial\omega$  of the object can be then parametrized by

$$\partial\omega = \left\{ \begin{pmatrix} x_0 \\ y_0 \end{pmatrix} + r(\theta) \begin{pmatrix} \cos \theta \\ \sin \theta \end{pmatrix}, \theta \in [0, 2\pi) \right\},$$

where  $x_0, y_0 \in \mathbb{R}$  and where  $r$  is a  $C^{1,1}$  function,  $2\pi$ -periodic and without double point. Taking into account of the ill-posedness of the problem, we approximate the polar radius  $r$  by its truncated Fourier series

$$r_N(\theta) := a_0^N + \sum_{k=1}^N a_k^N \cos(k\theta) + b_k^N \sin(k\theta),$$

for the numerical simulations. Indeed this regularization by projection permits to remove *high frequencies* generated by  $\cos(k\theta)$  and  $\sin(k\theta)$  for  $k \gg 1$ , for which the functional is degenerated. Then the unknown shape is entirely defined by the coefficients  $(a_i, b_i)$ . Hence, for  $k = 1, \dots, N$ , the corresponding deformation directions are respectively,

$$\mathbf{V}_1 := \mathbf{V}_{x_0} := \begin{pmatrix} 1 \\ 0 \end{pmatrix}, \quad \mathbf{V}_2 := \mathbf{V}_{y_0} := \begin{pmatrix} 0 \\ 1 \end{pmatrix}, \quad \mathbf{V}_3(\theta) := \mathbf{V}_{a_0}(\theta) := \begin{pmatrix} \cos \theta \\ \sin \theta \end{pmatrix},$$

$$\mathbf{V}_{2k+2}(\theta) := \mathbf{V}_{a_k}(\theta) := \cos(k\theta) \begin{pmatrix} \cos \theta \\ \sin \theta \end{pmatrix}, \quad \mathbf{V}_{2k+3}(\theta) := \mathbf{V}_{b_k}(\theta) := \sin(k\theta) \begin{pmatrix} \cos \theta \\ \sin \theta \end{pmatrix},$$

$\theta \in [0, 2\pi)$ . The gradient is then computed component by component using its characterization (see Proposition 3.1, formula (3.1)):

$$\left( \nabla \mathcal{K}_\varepsilon(\omega) \right)_k = D\mathcal{K}_\varepsilon(\omega) \cdot \mathbf{V}_k, \quad k = 1, \dots, 2N + 3.$$

### 3.3 Algorithm

The algorithm in this part is basically the same as the one for the data completion problem: we follow again a scheme of gradient algorithm but now we include also the modification of the shape of  $\omega$  which is updated on each iteration by the value of the shape derivative of our functional on each direction considered in the parametrization of  $\omega$ .

#### Algorithm

1. Let  $k = 0$ . Fix  $k_{max}$  (max. number of iterations) and  $tol$  (tolerance), choose  $(\varphi_0, \psi_0)$  as the initial guess of the missing data.
2. Solve problems (1.6) and (1.7) with  $(\omega_k, \varphi_k, \psi_k)$ , extract the solutions  $u_D^k(\omega_k, \varphi_k, \psi_k) := u_{\varphi_k}$ ,  $u_N^k(\omega_k, \varphi_k, \psi_k) := u_{\psi_k}$ ,  $v_D^k(\omega_k, \varphi_k, \psi_k) := v_{\varphi_k}$ ,  $v_N^k(\omega_k, \varphi_k, \psi_k) := v_{\psi_k}$  and compute  $\mathcal{K}(\omega_k, \varphi_k, \psi_k)$ .
  - If  $\mathcal{K}(\omega_k, \varphi_k, \psi_k) < tol$ : STOP.
  - Else: continue to next step.
3. Solve problems (2.22) (defined into  $\Omega \setminus \overline{\omega_k}$  with homogeneous Dirichlet condition over  $\partial\omega$ ), (3.2) and (3.3) with  $(\omega_k, \varphi_k, \psi_k)$ , extract the solutions  $w_N(\omega_k, \varphi_k, \psi_k)$ ,  $w_D(\omega_k, \varphi_k, \psi_k)$ ,  $\rho_D^u(\omega_k, \varphi_k, \psi_k)$ ,  $\rho_N^u(\omega_k, \varphi_k, \psi_k)$ ,  $\rho_D^v(\omega_k, \varphi_k, \psi_k)$  and  $\rho_N^v(\omega_k, \varphi_k, \psi_k)$ .

4. Compute the descent directions  $\tilde{\varphi}, \tilde{\psi}$  using formulas (2.23), (2.24) with  $(\varphi_k, \psi_k)$  and the solutions given in steps 2 and 3.
5. Compute  $\nabla\mathcal{K}_\varepsilon(\omega_k)$  using formula (3.1).
6. Update  $\varphi_k \leftarrow (\varphi_k - \alpha_1\tilde{\varphi}), \psi_k \leftarrow (\psi_k - \alpha_2\tilde{\psi}), \omega_k \leftarrow \omega_k - \alpha_3\nabla\mathcal{K}_\varepsilon(\omega_k)$ .
7. While  $k \leq k_{max}$  and  $\mathcal{K}_\varepsilon(\omega_k, \varphi_k, \psi_k) - \mathcal{K}_\varepsilon(\omega_{k-1}, \varphi_{k-1}, \psi_{k-1}) < tol$ , get back to the step 2,  $k \leftarrow k + 1$ .

As before, the step lengths  $\alpha_1, \alpha_2, \alpha_3$  are set as fixed parameters in our simulations with  $\alpha_1 = \alpha_2 = 0.01, \alpha_3 = 0.025$ , the maximum number of iterations  $k_{max}$  is set to 250 and the tolerance  $tol$  for the functional is set to 0.1. We precise that we here use the *adaptive method* described in [22, Section 4.3]. It consists in increasing gradually the number of parameters during the algorithm to a fixed final number of parameters. For example, if we want to work with nineteen parameters, we begin by working with two parameters during five iterations, then with three parameters (we add the radius) during five more iterations, and then we add two search parameters every fifteen iterations. The algorithm is then the same than the one described above only replacing step 4. by

$$\omega_k(1 : m) \leftarrow \omega_k(1 : m) - \alpha_i \nabla\mathcal{K}_\varepsilon(\Omega \setminus \overline{\omega_k})(1 : m),$$

where  $\omega_k(1 : m)$  represents the  $m$  first coefficients parametrizing the shape  $\omega_k$  (the same notation holds for  $\nabla\mathcal{K}_\varepsilon(\Omega \setminus \overline{\omega_k})(1 : m)$ ). The number  $m$  grows to the fixed final number of parameters following the procedure described previously.

To conclude, we precise that we use, as before, the finite elements library FREEFEM++ (see [37]) to make the simulations into this part and the noisy case has the same considerations, in particular the construction of noise, as the ones of the data completion part.

### 3.4 Numerical simulations

In our first series of simulations (with and without noise), we try to detect a disk centered in the origin with radius  $r = 0.25$ , this is  $\omega^* = D((0,0), 0.25)$ . We consider the initial object  $\omega_0$  as the disk centered in  $(-0.1, 0.1)$  with radius  $r = 0.20$ , this is:  $\omega_0 = D((-0.1, 0.1), 0.20)$ . The number of parameters is set to the maximum of 15. The detection is effective as shown in Figure 4 and Table 3 for the non noisy case and in Figure 5 and Table 4 for the noisy case (5%).

Table 3: Data completion for the object detection problem, non noisy case.

|                       |       | $\varepsilon = 0.1$ | $\varepsilon = 0.01$ | $\varepsilon = 0.001$ |
|-----------------------|-------|---------------------|----------------------|-----------------------|
| Approximated Center   |       | (-0.019,-0.006)     | (-0.022,-0.003)      | (-0.023,-0.002)       |
| $L^2(\Gamma_i)$ error | $u_D$ | 0.0958              | 0.0902               | 0.0899                |
|                       | $u_N$ | 0.0919              | 0.0927               | 0.0928                |

Table 4: Data completion for the object detection problem, noisy case (5%).

|                       |       | $\varepsilon = 0.1$ | $\varepsilon = 0.01$ | $\varepsilon = 0.001$ |
|-----------------------|-------|---------------------|----------------------|-----------------------|
| Approximated Center   |       | (-0.021,-0.017)     | (-0.021,-0.003)      | (-0.024,-0.001)       |
| $L^2(\Gamma_i)$ error | $u_D$ | 0.0998              | 0.0930               | 0.1033                |
|                       | $u_N$ | 0.0946              | 0.0935               | 0.0953                |

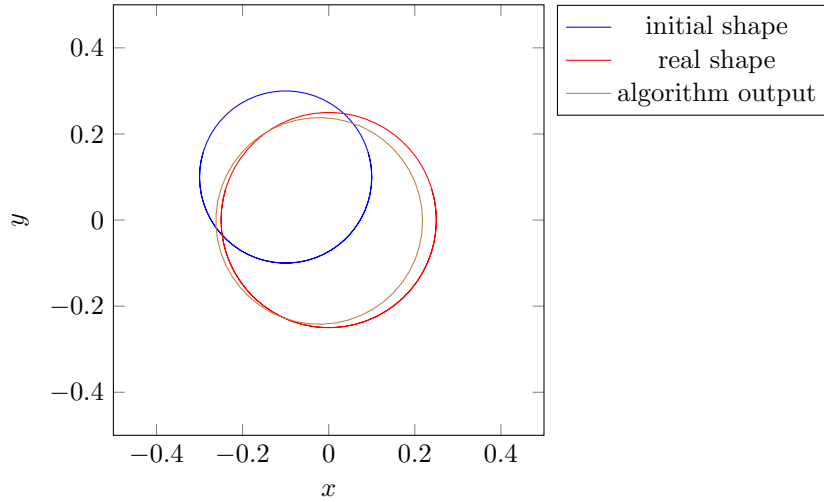


Figure 4: Object detection without noise: Real solution, initial guess and obtained obstacle ( $\varepsilon = 0.001$ ).

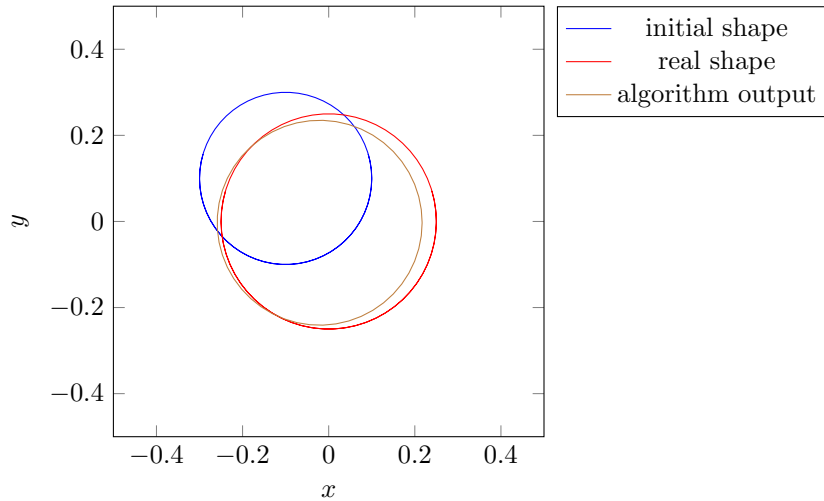


Figure 5: Object detection with noise (5%): Real solution, initial guess and obtained obstacle. ( $\varepsilon = 0.01$ ).

In a second series of simulations, we consider now a more complicated obstacle to test the method: we try to detect a square with relative center  $C = (0.0, -0.1)$  and side  $d = 0.4$ . The idea is to study the behavior of the method in the case where a non regular obstacle is introduced. The initial object  $\omega_0$  is set to be the disk centered in  $(0.0, 0.0)$  with radius  $r = 0.2$ , this is:  $\omega_0 = D((0.0, 0.0), 0.2)$ . As before, the number of parameters is set to the maximum of 15. Here again, we approximate the obstacle as underline in Figure 6 and Table 5 for the non noisy case and in Figure 7 and Table 6 for the noisy case (5%)

### 3.5 Comments on the simulations

These simulations show that our algorithm permits to correct the guess localization and shape of the introduced disk in order to obtain a better approximation of the real obstacle. Note that the algorithm is capable to detect that the number of active parameters could be wrong. Indeed, in the first series of simulations, the algorithm stops when it tries to

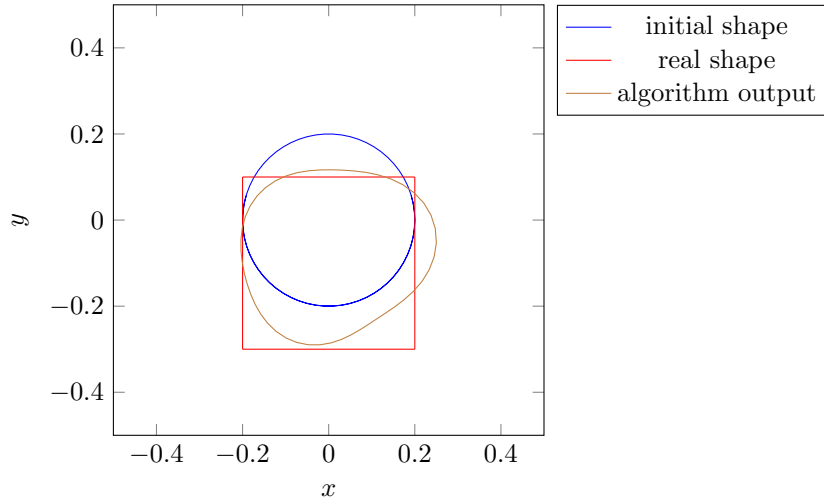


Figure 6: Object detection without noise: Real solution, initial guess and obtained obstacle ( $\varepsilon = 0.001$ )

Table 5: Data completion for the object detection problem, non-noisy case.

|                       |       | $\varepsilon = 0.1$ | $\varepsilon = 0.01$ | $\varepsilon = 0.001$ |
|-----------------------|-------|---------------------|----------------------|-----------------------|
| Relative Center       |       | (-0.000,-0.071)     | (-0.000,-0.082)      | (-0.000,-0.086)       |
| $L^2(\Gamma_i)$ error | $u_D$ | 0.0758              | 0.0688               | 0.0666                |
|                       | $u_N$ | 0.0901              | 0.0878               | 0.0869                |

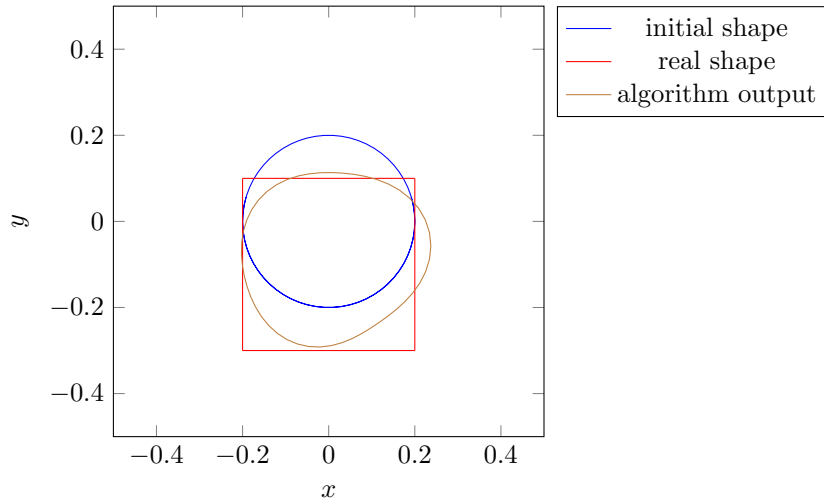


Figure 7: Object detection without noise: Real solution, initial guess and obtained obstacle ( $\varepsilon = 0.001$ ).

Table 6: Data completion for the object detection problem, noisy case (5%).

|                       |       | $\varepsilon = 0.1$ | $\varepsilon = 0.01$ | $\varepsilon = 0.001$ |
|-----------------------|-------|---------------------|----------------------|-----------------------|
| Relative Center       |       | (0.010,-0.067)      | (-0.001,-0.083)      | (-0.002,-0.088)       |
| $L^2(\Gamma_i)$ error | $u_D$ | 0.0888              | 0.0720               | 0.0641                |
|                       | $u_N$ | 0.0916              | 0.0895               | 0.0878                |

include more parameters than the real ones (only 3, as we are approximating a circle). In the second series of examples the algorithm continues until the inclusion of 9 parameters, which approximates better the corners and the relative area covered by the square.

### 3.6 Comparison with the case of complete boundary data

In this section, we compare descriptively our method against the case where we have full boundary data, this is, using the shape gradient algorithm with full boundary data. The idea is to compare the obtained results in order to have a better understanding of the capabilities of our proposed algorithm and their limitations.

In the case of full boundary data  $(g_D, g_N) \in H^{1/2}(\partial\Omega) \times H^{-1/2}(\partial\Omega)$ , we consider the following Kohn-Vogelius functional:

$$KV(\omega) = \frac{1}{2} \int_{\Omega \setminus \bar{\omega}} |\nabla(u_D(\omega) - u_N(\omega))|^2, \quad (3.6)$$

where  $u_D, u_N \in H^1(\Omega \setminus \bar{\omega})$  satisfy

$$\begin{cases} -\Delta u_D = 0 & \text{in } \Omega \setminus \bar{\omega} \\ u_D = g_D & \text{on } \partial\Omega \\ u_D = 0 & \text{on } \partial\omega, \end{cases} \quad \text{and} \quad \begin{cases} -\Delta u_N = 0 & \text{in } \Omega \setminus \bar{\omega} \\ \partial_\nu u_N = g_N & \text{on } \partial\Omega \\ u_N = 0 & \text{on } \partial\omega. \end{cases} \quad (3.7)$$

Moreover, the shape derivative of the Kohn-Vogelius functional  $KV$  for the shape  $\omega$  in the direction  $\mathbf{V} \in \mathbf{U}$  is given by:

$$DKV(\omega) \cdot \mathbf{V} = \int_{\partial\omega} \left( \partial_\nu(u_D - u_N) \cdot \partial_\nu u_D + \frac{1}{2} |\nabla(u_D - u_N)|^2 \right) (\mathbf{V} \cdot \nu). \quad (3.8)$$

Then we follow the same considerations as in Section 3.2, this is, we consider a polar coordinate parametrization of the boundary  $\partial\omega$  by means of a truncated Fourier series expansion of the polar radius and use the same perturbation directions  $\mathbf{V}$  proposed there. Hence we consider the following algorithm for the full boundary data case.

#### Algorithm

1. Let  $k = 0$ . Fix  $k_{max}$  (max. number of iterations),  $tol$  (tolerance) and  $\omega_0$ .
2. Solve problems (3.7) with  $\omega_k$ , extract the solutions  $u_D^k(\omega_k), u_N^k(\omega_k)$  and compute  $KV(\omega_k)$ .
  - If  $KV(\omega_k) < tol$ : STOP.
  - Else: continue to next step.
3. Compute  $\nabla KV(\omega_k)$  using formula (3.8),
4. Update  $\omega_k \leftarrow \omega_k - \alpha \nabla KV(\omega_k)$ .
5. While  $k \leq k_{max}$  and  $KV(\omega_k) - KV(\omega_{k-1}) < tol$ , get back to the step 2,  $k \leftarrow k + 1$ .

Finally, it is important to notice that in this case there is no regularization term since there is no completion data problem. However, the truncated Fourier series approximation for the unknown object boundary  $\partial\omega$  acts as a regularization method for this ill-posed inverse obstacle problem.

In this section, we consider the following example. Inside the exterior domain  $\Omega = [-1.0, 1.0] \times [-1.0, 1.0]$ , we want to detect the obstacle  $\omega^*$  such that their boundary  $\partial\omega^*$  is given by:

$$\partial\omega^* = \left\{ \left( \begin{array}{c} 0.05 \\ -0.20 \end{array} \right) + (0.40 - 0.05 \cos(\theta) + 0.05 \sin(\theta) - 0.20 \sin(2\theta)) \left( \begin{array}{c} \cos \theta \\ \sin \theta \end{array} \right), \theta \in [0, 2\pi) \right\}.$$

The real solution satisfies the overdetermined system:

$$\begin{cases} -\Delta u_{ex} = 0 & \text{in } \Omega \setminus \overline{\omega^*} \\ u_{ex} = g_D & \text{on } \partial\Omega \\ \partial_\nu u_{ex} = g_N & \text{on } \partial\Omega \\ u_{ex} = 0 & \text{on } \partial\omega^*, \end{cases} \quad (3.9)$$

where  $g_N = 1$  and  $g_D$  is constructed following the considerations given in Section 3.2. In the partial data case, we consider  $\Gamma_{obs}$  and  $\Gamma_i$  as defined in the previous examples and we set  $(\varphi_0, \psi_0) = (0.9, 1.0)$  and  $\varepsilon = 0.001$ .

In Figure 8, we can observe the behavior of both algorithms starting from the same guess  $\omega_0 = D((0.05, -0.50), 0.40)$ . The shape gradient with full boundary data provides very accurate results for this problem, this has been pointed out in several works and contexts (see for example [22]). On the other hand our algorithm provides interesting results in this case, the obtained shape is similar in the regions close to the boundary where Cauchy data is available  $\Gamma_{obs}$  however it tends to be of lower quality in the border which is closer to the upper boundary of the square, this is, in the inaccessible region  $\Gamma_i$ . However, we have similar defects as the full boundary data algorithm in the regions close to the observable boundary.

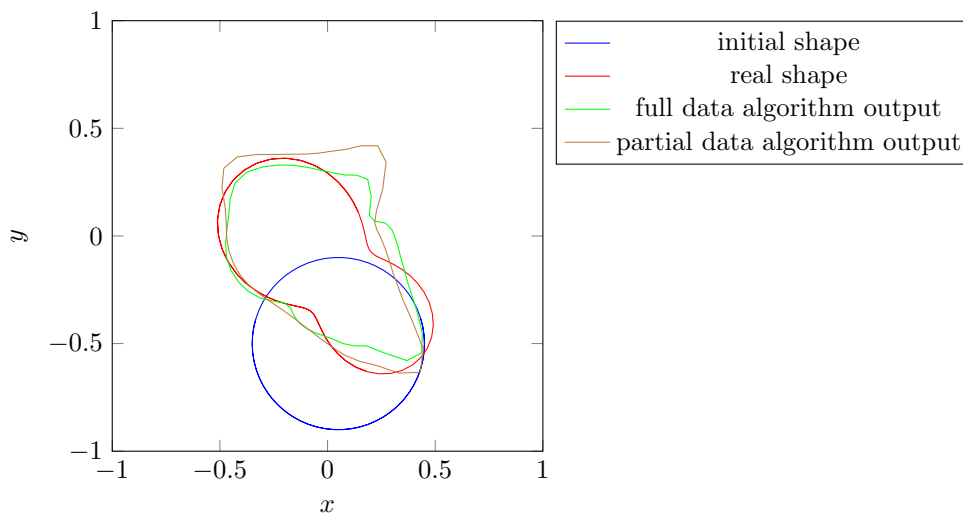


Figure 8: Comparison between algorithms in the non noisy case.

The noisy case shows (see Figure 9), as we have seen in the previous examples, that our algorithm is robust and permits to obtain similar results even when the data  $(g_N, g_D)$  is polluted with a moderated amount of noise ( $\sigma = 5\%$ ).

## 4 Conclusion

Using a Kohn-Vogelius approach, we have performed the detection of an obstacle immersed in a two dimensional domain governed by Laplace's equation by means of partial bound-

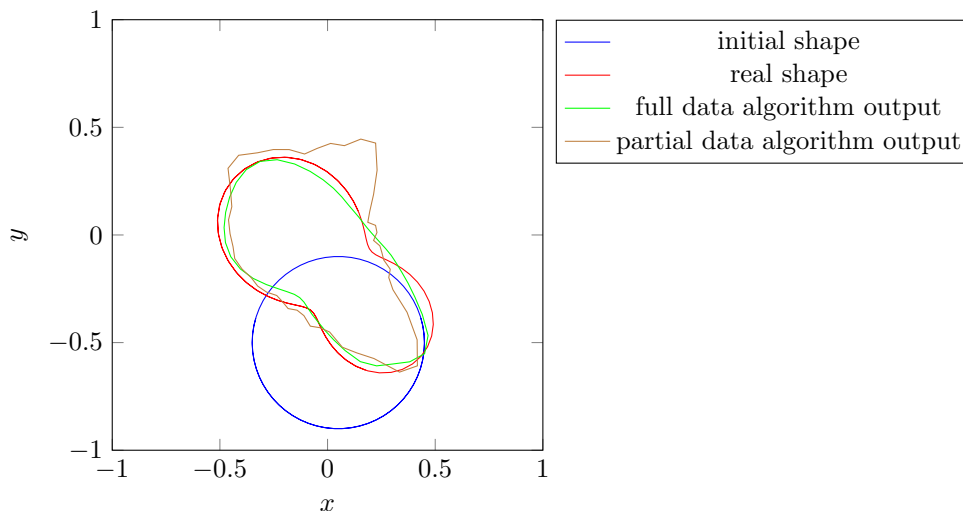


Figure 9: Comparison between algorithms in the noisy case (5%).

ary measurements  $(g_N, g_D)$  on an accessible part of the boundary  $\Gamma_{obs} \subsetneq \partial\Omega$ . We have proposed a functional which consider several unknowns: the obstacle  $\omega$  and the inaccessible data  $(\varphi, \psi)$  on the inaccessible part of the boundary  $\Gamma_i$ . The minimization of this functional is then equivalent to solve two ill-posed problems: the data completion problem and the obstacle detection problem. Concerning the data completion problem, we have obtained several results such as the existence of a solution and we have introduced a Tikhonov regularization in order to deal with the ill-posedness of the problem, obtaining several convergence properties to the real solution even when only noisy data is available. Finally we have proposed an algorithm to solve the inverse obstacle problem with partial boundary data which combines the data completion part and a shape optimization part using gradient algorithms. We obtain good reconstructions and compare these results with the full boundary data case.

## Acknowledgements

The authors thank partial support from ECOS-CONICYT Grant C13E05. The third author is partially supported by CONICYT-PCHA/Doctorado Nacional/2012 and PIA-CONICYT grant FB-0001.

## References

- [1] J. Abouchabaka and C. Tajani. An alternating KMF algorithm to solve the Cauchy problem for Laplaces equation. *arXiv preprint arXiv:1405.3235*, 2014.
- [2] R. Aboulaich, A. B. Abda, and M. Kallel. A control type method for solving the Cauchy–Stokes problem. *Applied Mathematical Modelling*, 37(6):4295–4304, 2013.
- [3] L. Afraites, M. Dambrine, K. Eppler, and D. Kateb. Detecting perfectly insulated obstacles by shape optimization techniques of order two. *Discrete Contin. Dyn. Syst. Ser. B*, 8(2):389–416 (electronic), 2007.

- [4] G. Alessandrini, E. Beretta, E. Rosset, and S. Vessella. Optimal stability for inverse elliptic boundary value problems with unknown boundaries. *Annali della Scuola Normale Superiore di Pisa - Classe di Scienze*, 29(4):755–806, 2000.
- [5] S. Amstutz. The topological asymptotic for the Navier-Stokes equations. *ESAIM Control Optim. Calc. Var.*, 11(3):401–425 (electronic), 2005.
- [6] S. Andrieux, T. Baranger, and A. B. Abda. Solving Cauchy problems by minimizing an energy-like functional. *Inverse problems*, 22(1):115, 2006.
- [7] M. Azaïez, F. B. Belgacem, and H. El Fekih. On Cauchy’s problem: II. Completion, regularization and approximation. *Inverse problems*, 22(4):1307, 2006.
- [8] M. Badra, F. Caubet, and M. Dambrine. Detecting an obstacle immersed in a fluid by shape optimization methods. *Math. Models Methods Appl. Sci.*, 21(10):2069–2101, 2011.
- [9] F. B. Belgacem. Why is the Cauchy problem severely ill-posed? *Inverse Problems*, 23(2):823, 2007.
- [10] F. B. Belgacem and H. El Fekih. On Cauchy’s problem: I. A variational Steklov–Poincaré theory. *Inverse Problems*, 21(6):1915, 2005.
- [11] F. B. Belgacem, H. El Fekih, and F. Jelassi. The Lavrentiev regularization of the data completion problem. *Inverse Problems*, 24(4):045009, 2008.
- [12] F. B. Belgacem, H. El Fekih, and F. Jelassi. The Lavrentiev regularization of the data completion problem. *Inverse Problems*, 24(4):045009, 2008.
- [13] L. Bourgeois and J. Dardé. A duality-based method of quasi-reversibility to solve the Cauchy problem in the presence of noisy data. *Inverse Problems*, 26(9):095016, 2010.
- [14] L. Bourgeois and J. Dardé. About stability and regularization of ill-posed elliptic Cauchy problems: the case of Lipschitz domains. *Applicable Analysis*, 89(11):1745–1768, 2010.
- [15] L. Bourgeois and J. Dardé. A quasi-reversibility approach to solve the inverse obstacle problem. *Inverse Probl. Imaging*, 4(3):351–377, 2010.
- [16] H. Brezis. *Analyse fonctionnelle*. Collection Mathématiques Appliquées pour la Maîtrise. [Collection of Applied Mathematics for the Master’s Degree]. Masson, Paris, 1983. Théorie et applications. [Theory and applications].
- [17] D. Bucur and G. Buttazzo. *Variational methods in shape optimization problems*. Progress in Nonlinear Differential Equations and their Applications, 65. Birkhäuser Boston Inc., Boston, MA, 2005.
- [18] M. Burger and S. J. Osher. A survey on level set methods for inverse problems and optimal design. *European J. Appl. Math.*, 16(2):263–301, 2005.
- [19] E. Burman. A stabilized nonconforming finite element method for the elliptic Cauchy problem. *Math. Comp.*, 86(303):75–96, 2017.
- [20] F. Caubet, C. Conca, and M. Godoy. On the detection of several obstacles in 2d stokes flow: Topological sensitivity and combination with shape derivatives. *Inverse Problems and Imaging*, 10(2):327–367, 2016.



- [21] F. Caubet, M. Dambrine, and D. Kateb. Shape optimization methods for the inverse obstacle problem with generalized impedance boundary conditions. *Inverse Problems*, 29(11):115011, 26, 2013.
- [22] F. Caubet, M. Dambrine, D. Kateb, and C. Z. Timimoun. A Kohn-Vogelius formulation to detect an obstacle immersed in a fluid. *Inverse Probl. Imaging*, 7(1):123–157, 2013.
- [23] A. Cimetiere, F. Delvare, M. Jaoua, and F. Pons. Solution of the Cauchy problem using iterated Tikhonov regularization. *Inverse Problems*, 17(3):553, 2001.
- [24] D. Colton and R. Kress. *Inverse acoustic and electromagnetic scattering theory*, volume 93 of *Applied Mathematical Sciences*. Springer-Verlag, Berlin, second edition, 1998.
- [25] M. Dambrine. On variations of the shape Hessian and sufficient conditions for the stability of critical shapes. *RACSAM Rev. R. Acad. Cienc. Exactas Fís. Nat. Ser. A Mat.*, 96(1):95–121, 2002.
- [26] J. Dardé. *Quasi-reversibility and level set methods applied to elliptic inverse problems*. Theses, Université Paris-Diderot - Paris VII, Dec. 2010.
- [27] J. Dardé. Iterated quasi-reversibility method applied to elliptic and parabolic data completion problems. *arXiv preprint arXiv:1503.08641*, 2015.
- [28] M. Di Cristo and L. Rondi. Examples of exponential instability for inverse inclusion and scattering problems. *Inverse Problems*, 19(3):685–701, 2003.
- [29] H. W. Engl, M. Hanke, and A. Neubauer. *Regularization of inverse problems*, volume 375. Springer Science & Business Media, 1996.
- [30] A. V. Fursikov. *Optimal control of distributed systems. Theory and applications*. American Mathematical Soc., 1999.
- [31] M. Godoy. *The inverse problem of obstacle detection via optimization methods*. Thesis, Universidad de Chile, July 2016.
- [32] P. Guillaume and K. Sid Idris. The topological asymptotic expansion for the Dirichlet problem. *SIAM J. Control Optim.*, 41(4):1042–1072 (electronic), 2002.
- [33] P. Guillaume and K. Sid Idris. Topological sensitivity and shape optimization for the Stokes equations. *SIAM J. Control Optim.*, 43(1):1–31 (electronic), 2004.
- [34] J. Hadamard. *Le probleme de Cauchy et les équations aux dérivées partielles linéaires hyperboliques*, volume 220. Paris, 1932.
- [35] H. Haddar and R. Kress. Conformal mappings and inverse boundary value problems. *Inverse Problems*, 21(3):935–953, 2005.
- [36] H. Han, L. Ling, and T. Takeuchi. An energy regularization for Cauchy problems of Laplace equation in annulus domain. *Communications in Computational Physics*, 9(4):878, 2011.
- [37] F. Hecht. Finite Element Library FREEFEM++. <http://www.freefem.org/ff++/>.

- [38] A. Henrot and M. Pierre. *Variation et optimisation de formes*, volume 48 of *Mathématiques & Applications (Berlin) [Mathematics & Applications]*. Springer, Berlin, 2005. Une analyse géométrique. [A geometric analysis].
- [39] V. A. Kozlov, V. G. Maz'ya, and A. Fomin. An iterative method for solving the Cauchy problem for elliptic equations. *Zhurnal Vychislitel'noi Matematiki i Matematicheskoi Fiziki*, 31(1):64–74, 1991.
- [40] R. Kress and W. Rundell. Nonlinear integral equations and the iterative solution for an inverse boundary value problem. *Inverse Problems*, 21(4):1207–1223, 2005.
- [41] J. Leblond and D. Ponomarev. Recovery of harmonic functions from partial boundary data respecting internal pointwise values. *J. Inverse Ill-Posed Probl.*, 25(2):157–174, 2017.
- [42] F. Murat and J. Simon. *Sur le contrôle par un domaine géométrique*. Rapport du L.A. 189, 1976. Université de Paris VI, France.
- [43] R. Potthast. A survey on sampling and probe methods for inverse problems. *Inverse Problems*, 22(2):R1–R47, 2006.
- [44] W. Rundell. Recovering an obstacle using integral equations. *Inverse Probl. Imaging*, 3(2):319–332, 2009.
- [45] G. Savaré. Regularity and perturbation results for mixed second order elliptic problems. *Communications in Partial Differential Equations*, 22(5-6):869–899, 1997.
- [46] J. Simon. Differentiation with respect to the domain in boundary value problems. *Numer. Funct. Anal. Optim.*, 2(7-8):649–687 (1981), 1980.
- [47] J. Simon. Second variations for domain optimization problems. In *Control and estimation of distributed parameter systems (Vorau, 1988)*, volume 91 of *Internat. Ser. Numer. Math.*, pages 361–378. Birkhäuser, Basel, 1989.
- [48] J. Sokołowski and J.-P. Zolésio. *Introduction to shape optimization*, volume 16 of *Springer Series in Computational Mathematics*. Springer-Verlag, Berlin, 1992. Shape sensitivity analysis.